July 17, 2012
Workshop on Building Collaborations
in Clouds, HPC, and Application Areas

Computing in Hydrology: data analysis, numerical modeling and computational technology

Dr. Ji CHEN
Department of Civil Engineering
The University of Hong Kong, Pokfulam
Hong Kong, China

The University of Hong Kong

JOURNAL OF GEOPHYSICAL RESEARCH, VOL. 115, G00H04, doi:10.1029/2009JG001246, 2010

Using MODIS EVI to detect vegetation damage caused by the 2008 ice and snow storms in south China

Ji Chen[1] and Liqun Sun[1]

Received 30 November 2009; revised 4 July 2010; accepted 7 July 2010; published 29 October 2010.

[1] This study develops a new method for detecting areas with severe vegetation damage caused by a serious ice and snow storm event that occurred in southern China over the period of 10 January to 2 February 2008. The new method adopts one of the Moderate Resolution Imaging Spectroradiometer (MODIS) MOD13A1 products, the enhanced vegetation index (EVI). Using a series of 16 day EVI maps at the 500 m spatial resolution

Data Analysis

Stoch Environ Res Risk Assess (2011) 25:555–565
DOI 10.1007/s00477-010-0421-0

ORIGINAL PAPER

Regional climate change and local urbanization effects on weather variables in Southeast China

Ji Chen · Qinglan Li · Jun Niu · Liqun Sun

JOURNAL OF GEOPHYSICAL RESEARCH, VOL. 115, G00H04, doi:10.1029/2009JG001246, 2010

Using MODIS EVI to detect vegetation damage caused by the 2008 ice and snow storms in south China

Ji Chen[1] and Liqun Sun[1]

Received 30 November 2009; revised 4 July 2010; accepted 7 July 2010; published 29 October 2010.

[1] This study develops a new method for detecting areas with severe vegetation damage caused by a serious ice and snow storm event that occurred in southern China over the period of 10 January to 2 February 2008. The new method adopts one of the Moderate Resolution Imaging Spectroradiometer (MODIS) MOD13A1 products, the enhanced vegetation index (EVI). Using a series of 16 day EVI maps at the 500 m spatial resolution

The shaded areas present the different numbers of freezing days during the 2008 ice/snow storm event in South China.

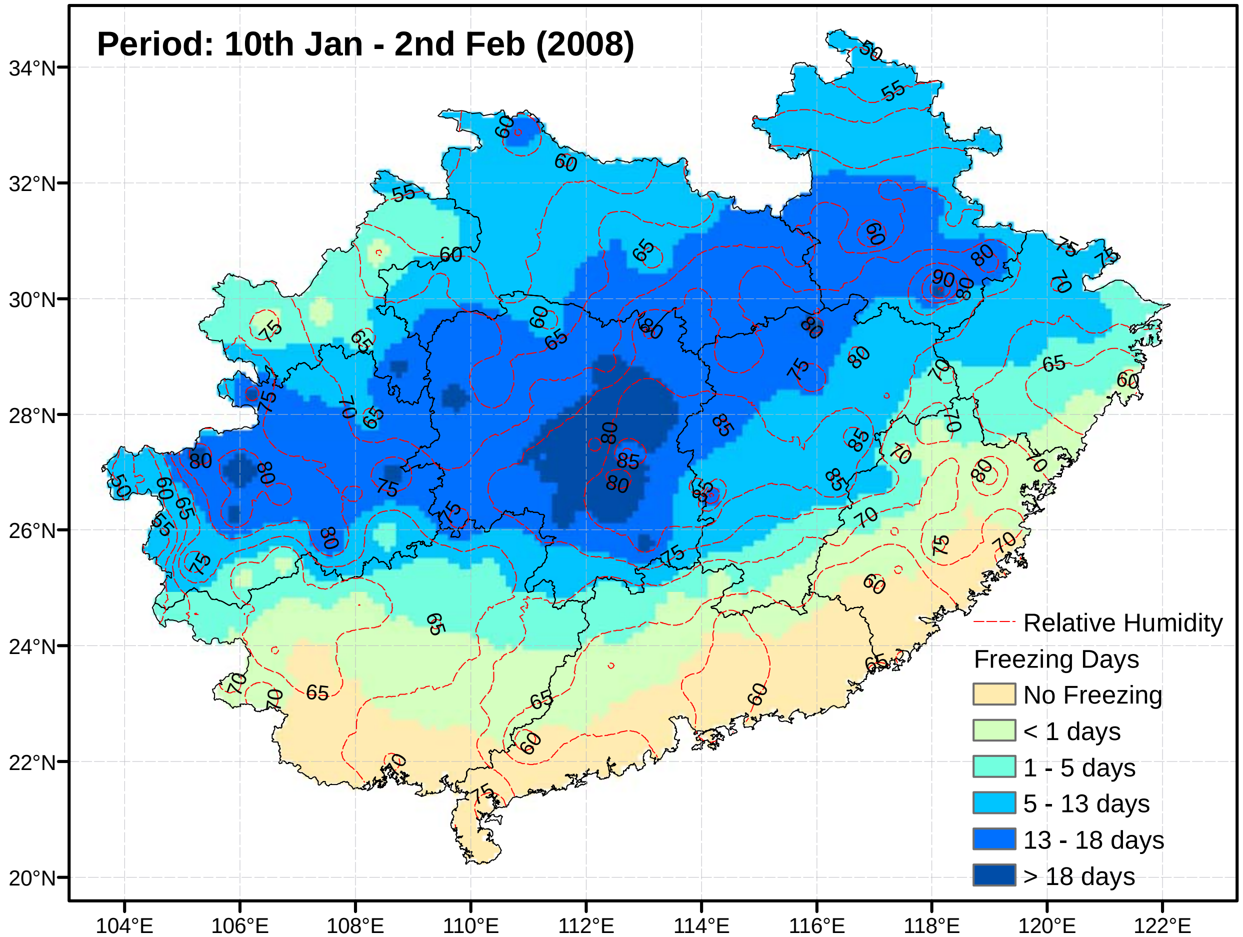

The **enhanced vegetation index** (EVI) is an 'optimized' index designed to enhance the vegetation signal with improved sensitivity in high biomass regions and improved vegetation monitoring through a de-coupling of the canopy background signal and a reduction in atmosphere influences

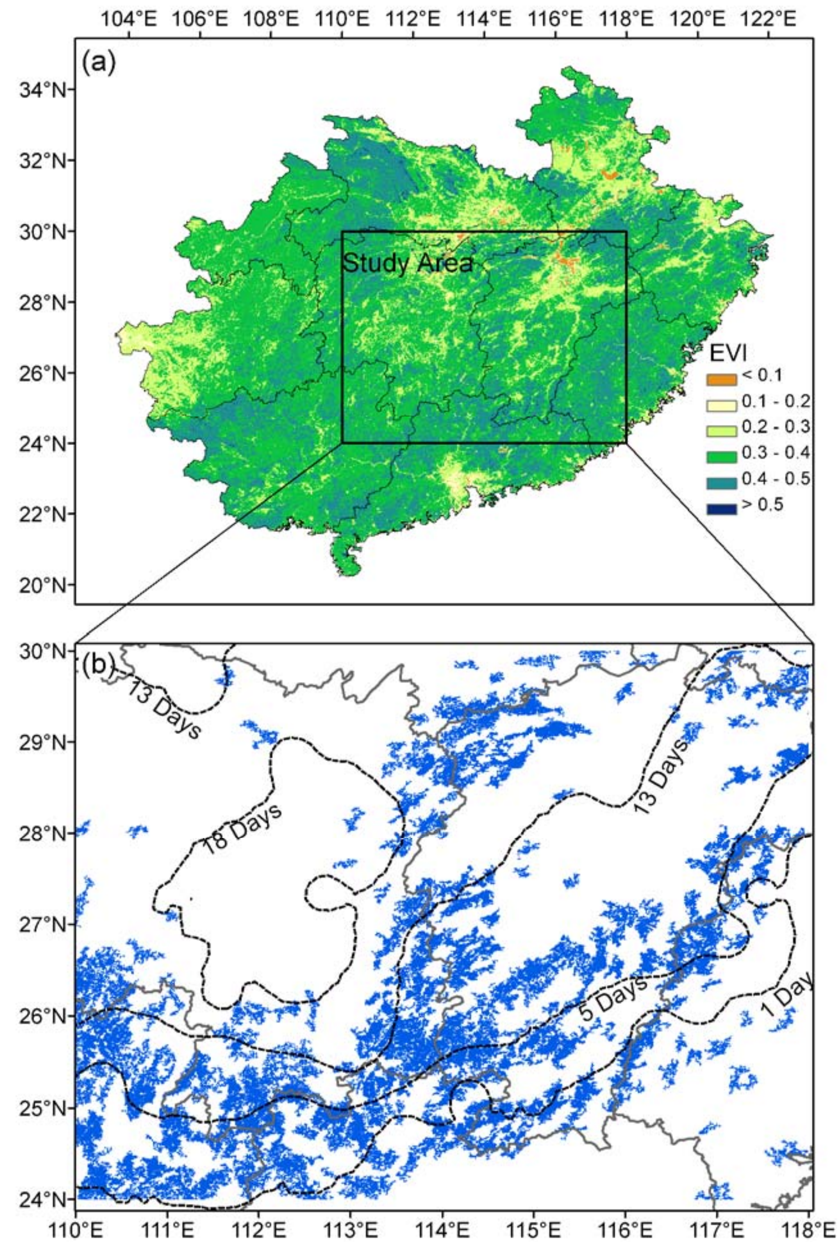

Delineation of Extensive Vegetation-Impacted Areas

$$\bar{e}(i)=\frac{1}{7}\sum_{j=1}^{7}EVI(i,DOY(81+(j-1)\times 16))\qquad i=2000,\cdots,2008$$

$$\bar{E}=\frac{1}{8}\sum_{i=2000}^{2007}\bar{e}(i)$$

$$E_{2008anomaly}=\bar{e}(2008)-\bar{E}$$

$$E_{std}=\sqrt{\frac{1}{8-1}\sum_{i=2000}^{2007}\left(\bar{e}(i)-\bar{E}\right)^2}$$

where *j* is one of seven EVI study phases (*i.e.*, DOY81, DOY97, DOY113, DOY129, DOY145, DOY161 and DOY177 phases).

(a) Average EVI values over the EVI study period were calculated, and the rectangular is the location of the study area (latitude between 24° N and 30° N, and longitude between 110° E and 118° E) in South China. (b) The shaded areas are the Extensive Vegetation-Impacted Areas (EVIAs), and the contour lines represent the number of freezing days.

Delineation of Severe Vegetation-Impacted Areas

$$\bar{S}(j) = \frac{1}{8}\sum_{i=2000}^{2007} EVI(i, DOY(81 + (j-1)\times 16)), \quad j = 1, \cdots, 7$$

$$S_{anomaly}(i, j) = EVI(i, DOY(81 + (j-1)\times 16)) - \bar{S}(j), \quad i = 2000, \cdots, 2008$$

$$S_{std}(j) = \sqrt{\frac{1}{8-1}\sum_{i=2000}^{2007}\left(EVI(i, DOY(81 + (j-1)\times 16)) - \bar{S}(j)\right)^2}$$

where is the average EVI at phase *j* over the period of 2000 to 2007.

$S_{anomaly}(i, j)$ and $S_{std}(j)$ are related EVI anomaly and standard deviation.

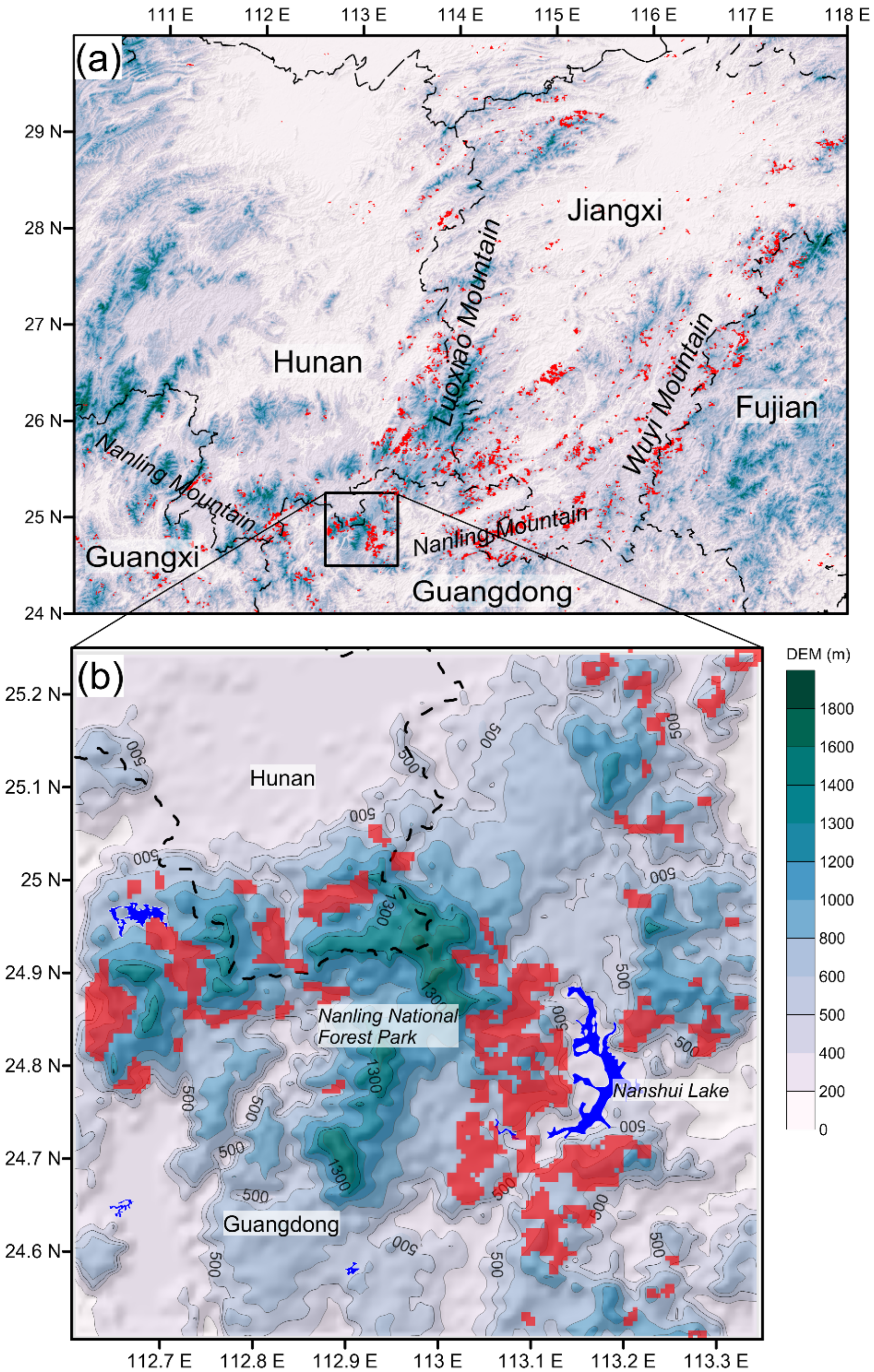

The distribution of Severe Vegetation-Impacted Areas (SVIAs) shaded in the Study Area and (b) a zoom in view of the SVIAs in Nanling National Forest Park (NNFP).

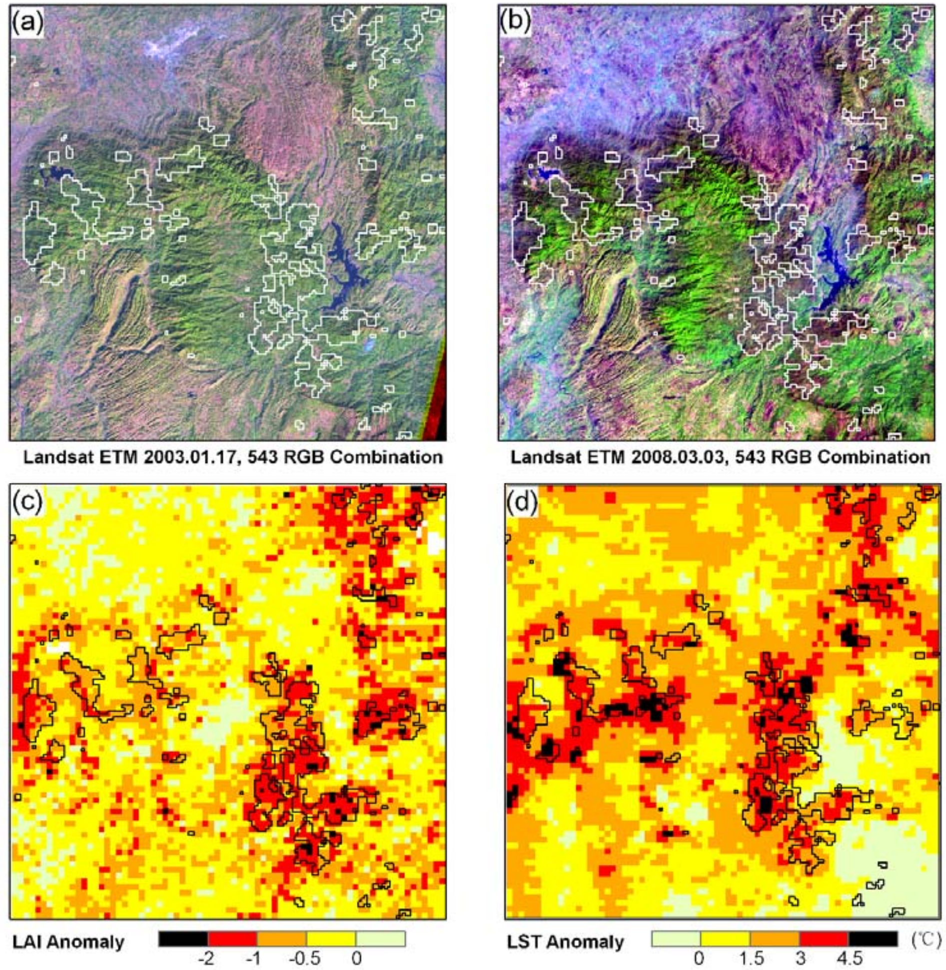

Confirmation of the vegetation damages in the SVIAs. (a) Landsat 7 ETM pre-storm image of Path 123 Row 043 acquired on 17 Jan. (b) Landsat 7 ETM post-storm image of Path 123 Row 043 acquired on 3 March 2008. The influence of SLC-off problem (see the text for the details) was removed. (c) and (d) are the 2008 Leaf Area Index (LAI) and Land Surface Temperature (LST) anomalies for the period of DOY81 to DOY192, respectively.

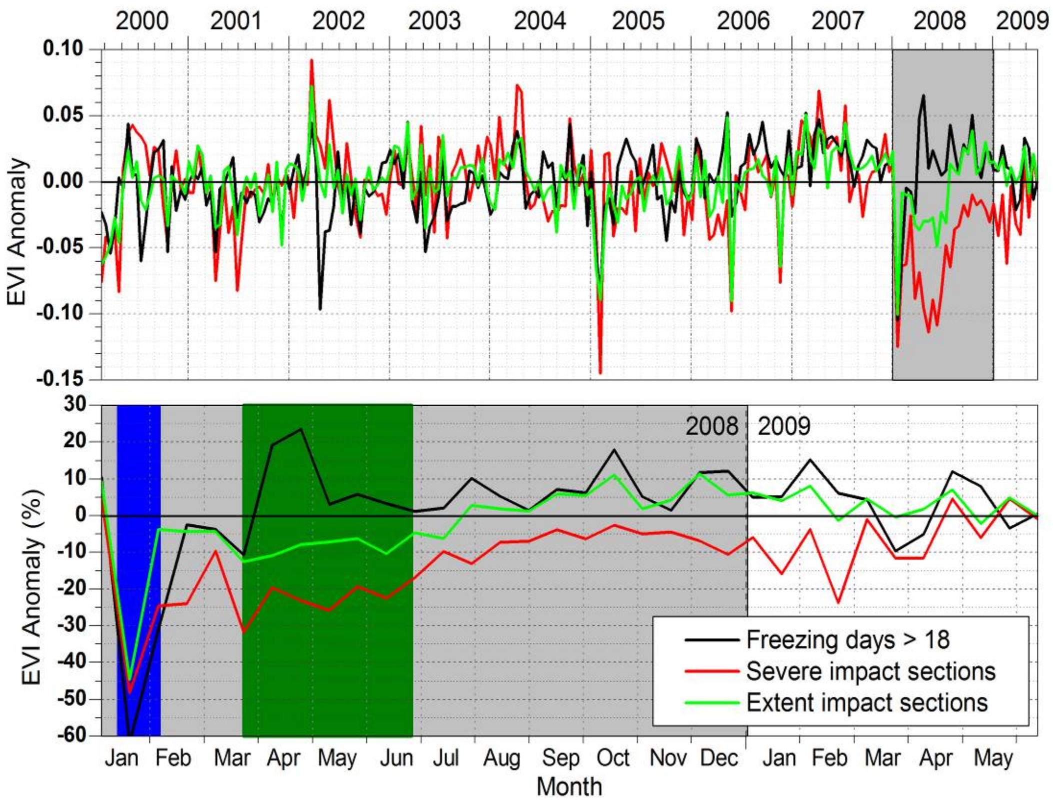

2000
2001
2002
2003
2004
2005
2006
2007
2008
2009
EVI Anomaly
EVI Anomaly (%)
Freezing days > 18
Severe impact sections
Extent impact sections
Jan
Feb
Mar
Apr
May
Jun
Jul
Aug
Sep
Oct
Nov
Dec
Month

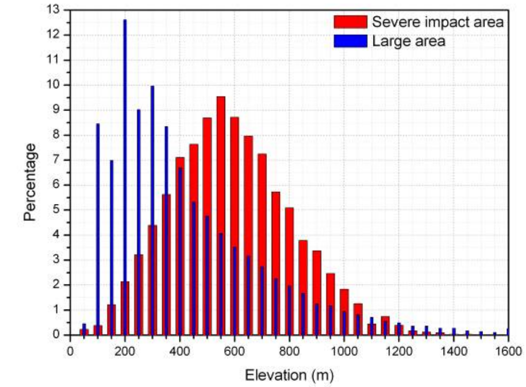

Severe impact area
Large area
Percentage
Elevation (m)

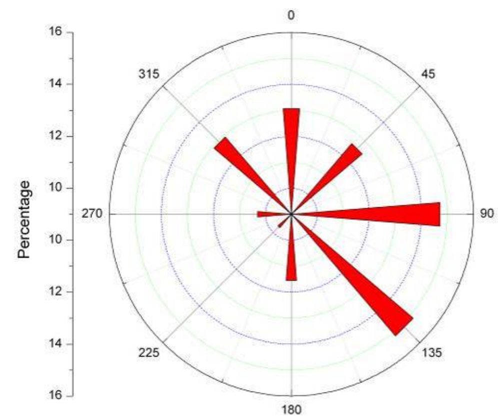

Percentage

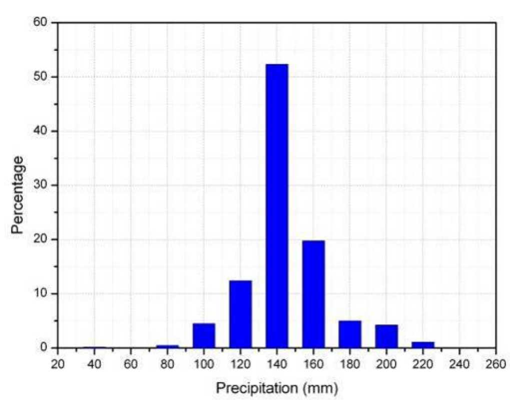

Percentage
Precipitation (mm)

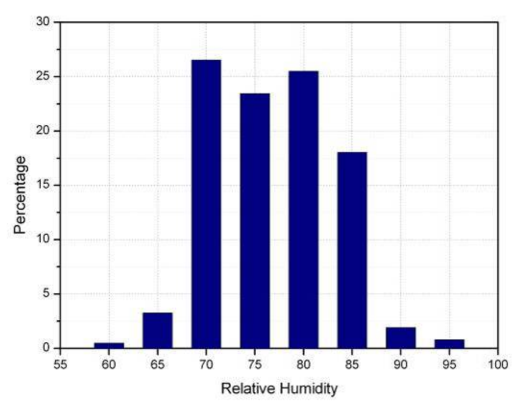

Percentage
Relative Humidity

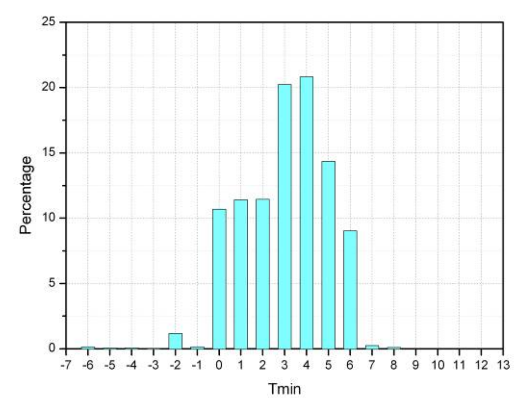

Percentage
Tmin

Stoch Environ Res Risk Assess (2011) 25:555–565
DOI 10.1007/s00477-010-0421-0

ORIGINAL PAPER

Regional climate change and local urbanization effects on weather variables in Southeast China

Ji Chen · Qinglan Li · Jun Niu · Liqun Sun

Area interested and Dataset (1960 to 2005)

Latitude: 21^{o}N~25^{o}N

Longitude: 111^{o}E~116^{o}E

21 stations involved

- **Data:** from 1960 to 2005

  Monthly average of daily Tmax, Tmin, precipitation, relative humidity

(from: Chinese National Meteorological Center)

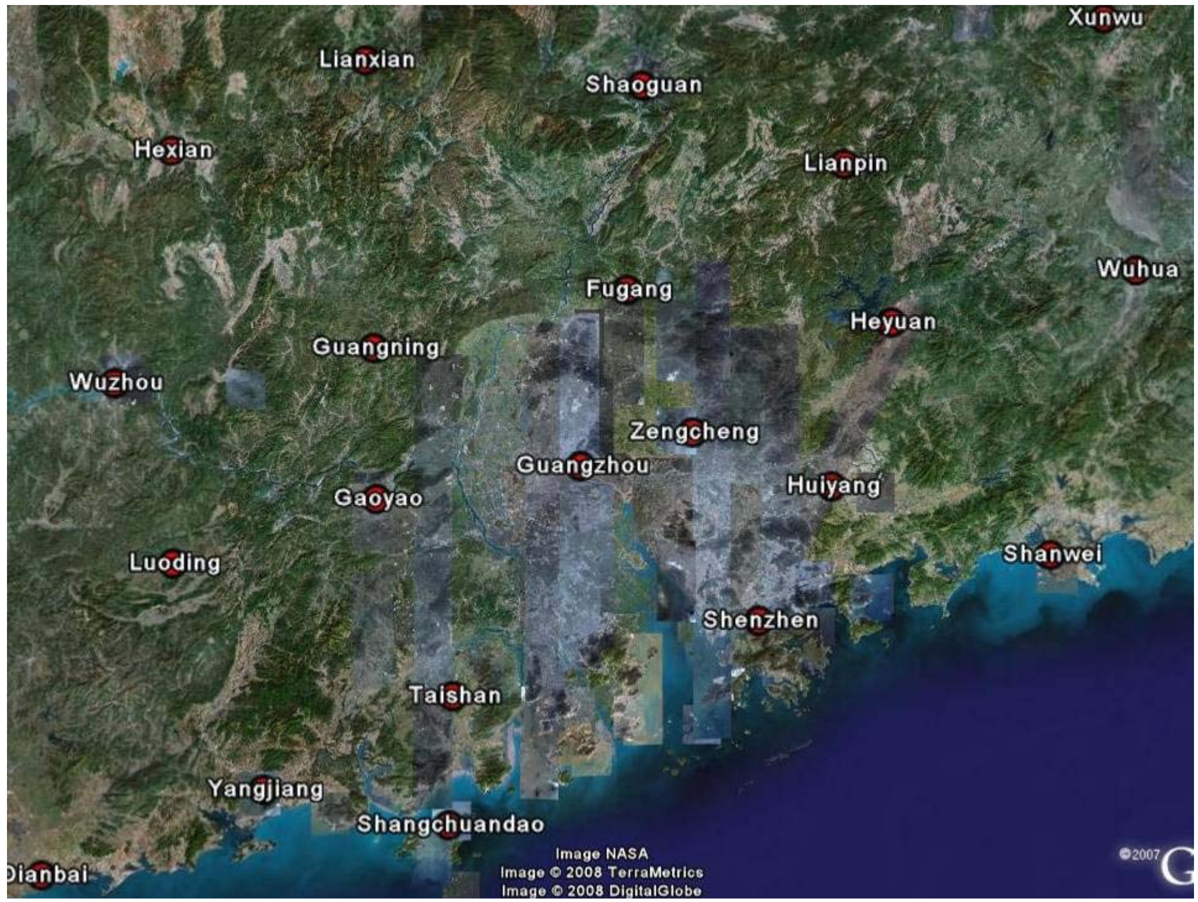

land use in 1980 and Locations of 21 measuring stations

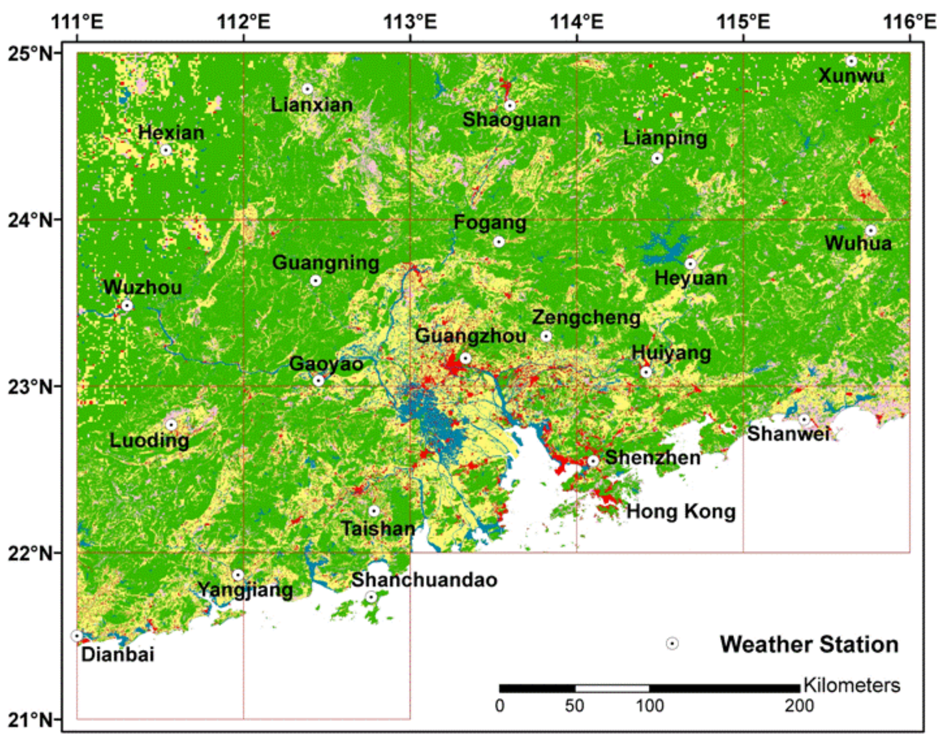

land use in 2000 and 17 grids with resolution 1°×1°

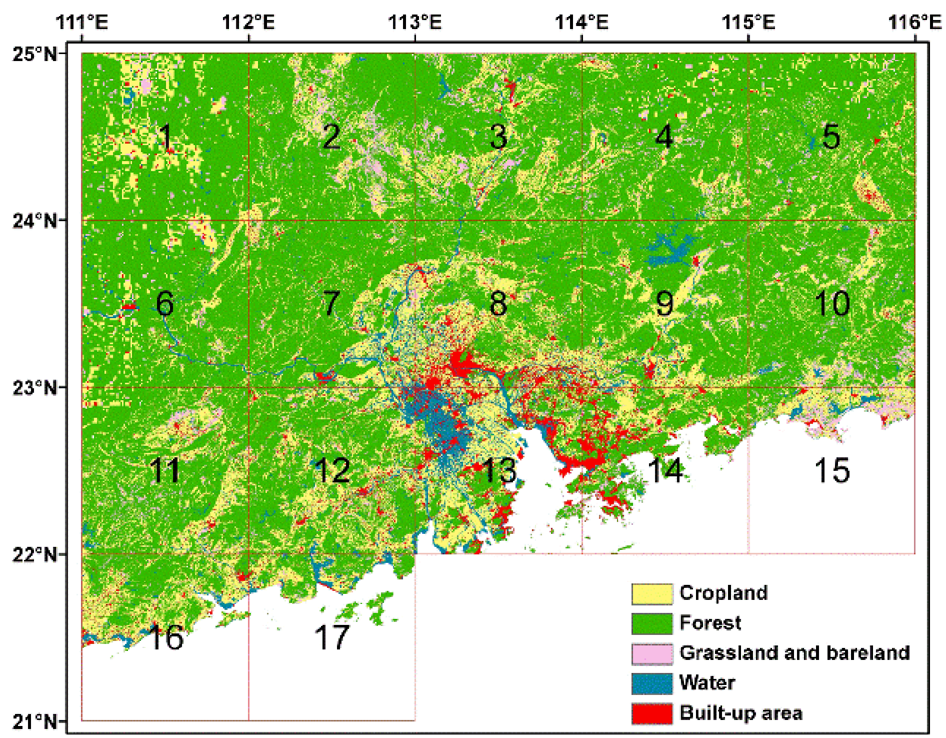

comparison of population and built-up area from 1983 to 2005 in the Fast Developing Cities (FDC) and Slow Developing Cities (SDC)

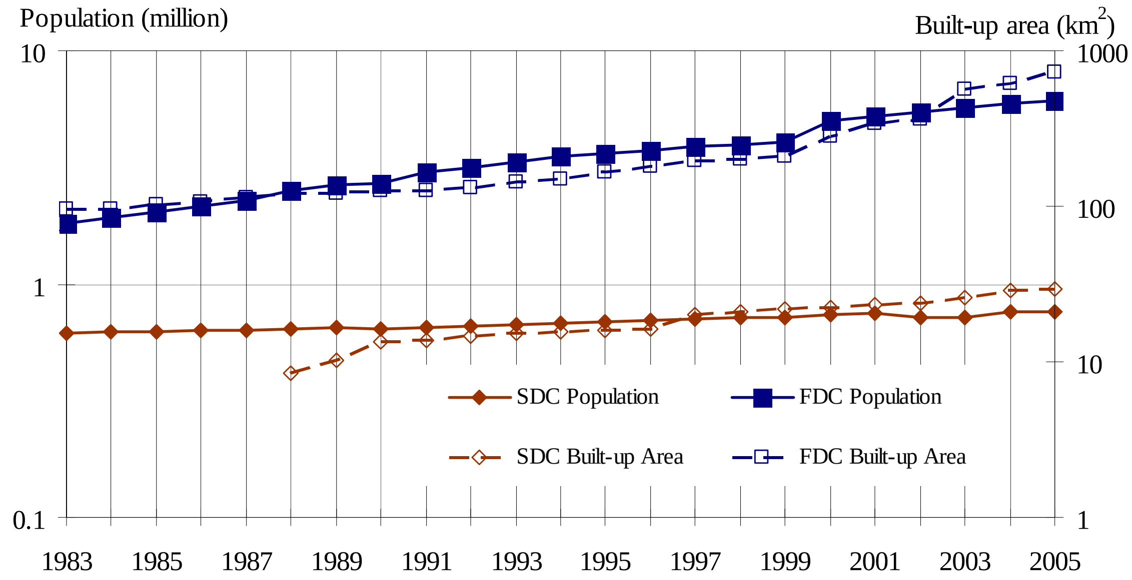

the percentage of land cover changes of built-up area and cropland for 17 1º×1º grids

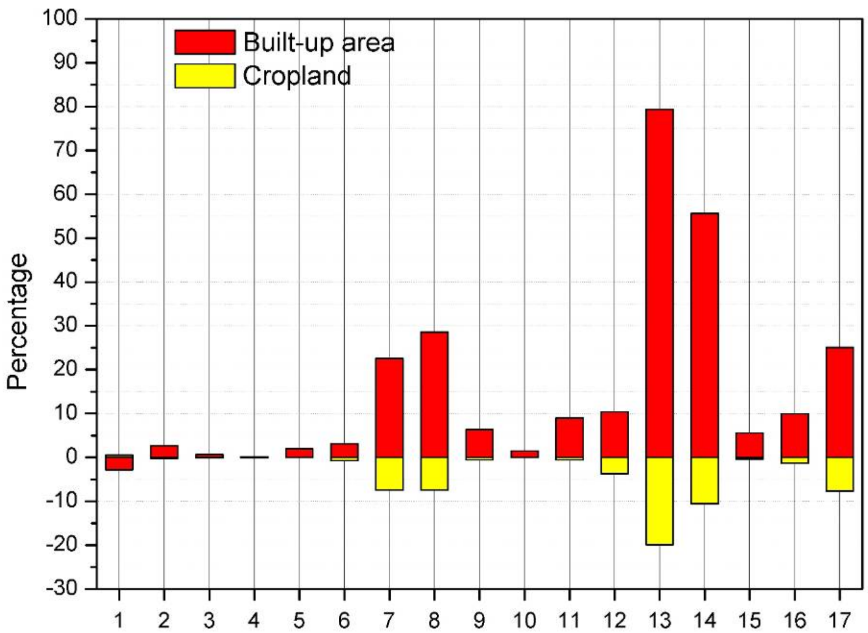

annual time series of the anomalies of the Tmin

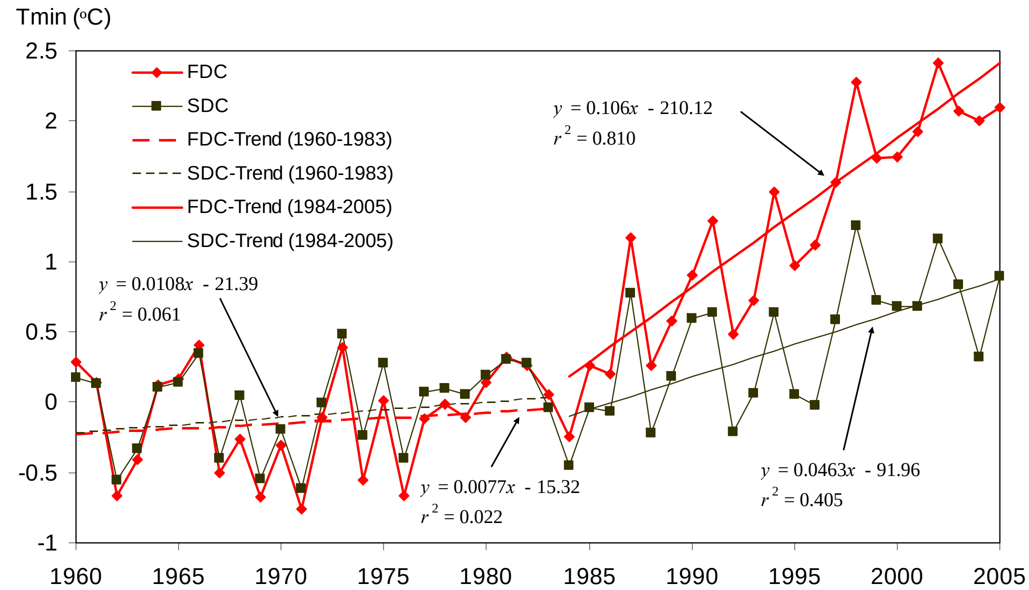

annual time series of the anomalies of the Tmax

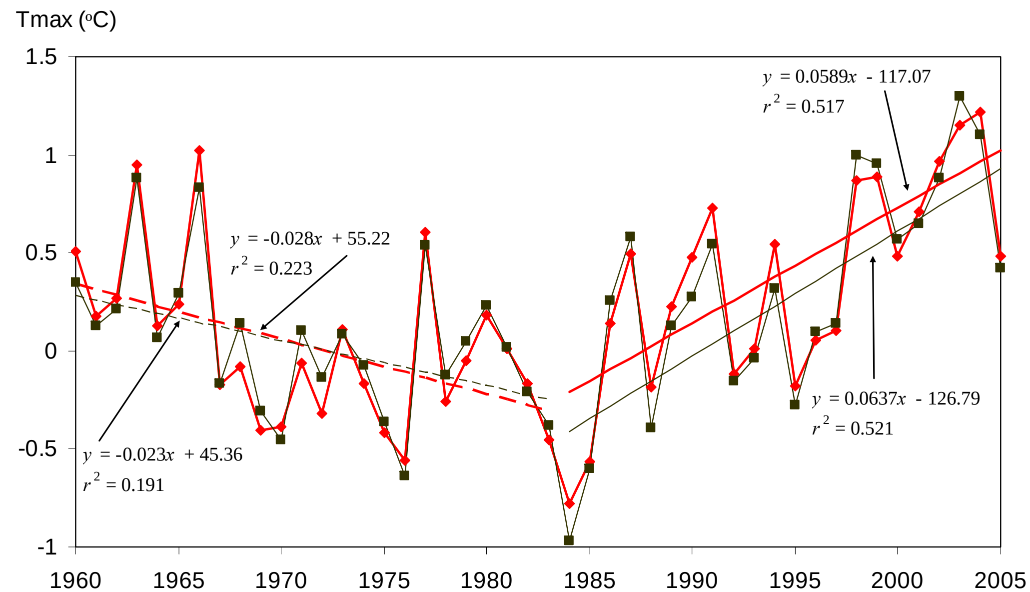

annual time series of the anomalies of the RH

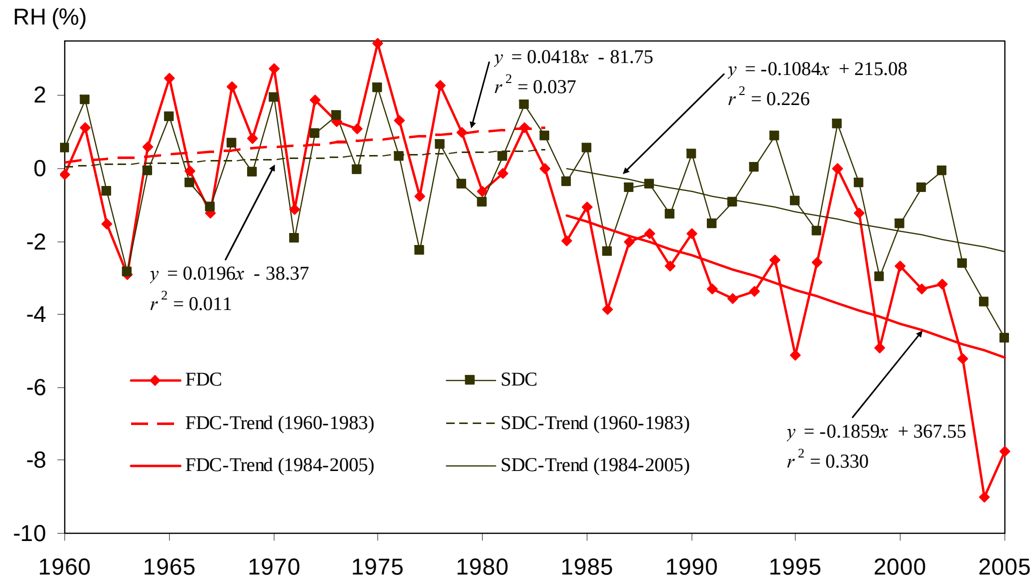

annual time series of the anomalies of the P

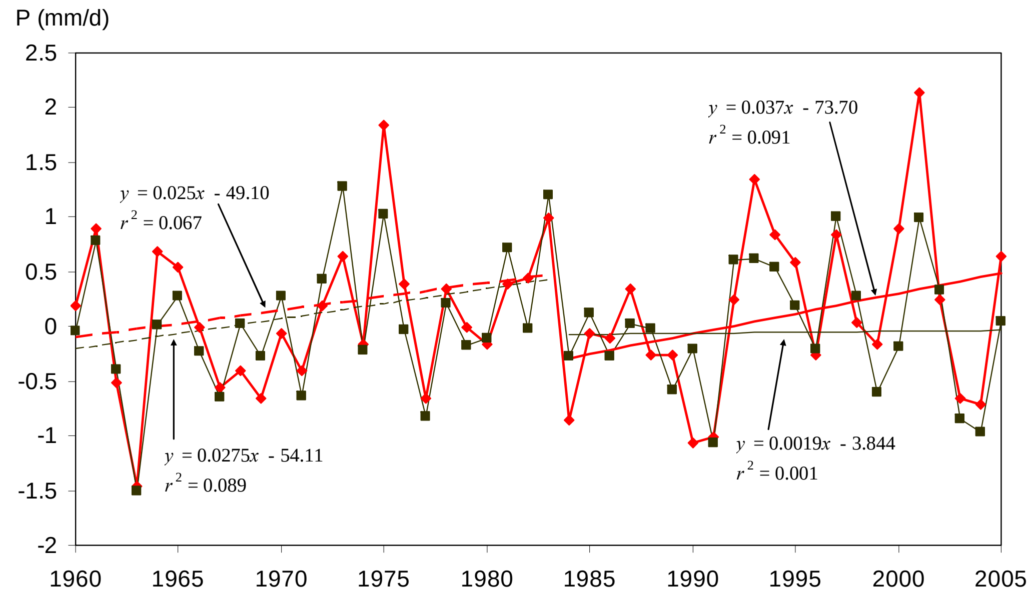

Available online at www.sciencedirect.com

ScienceDirect

Journal of Hydro-environment Research 4 (2010) 279–288

Journal of Hydro-environment Research

www.elsevier.com/locate/jher

Research paper

Terrestrial hydrological features of the Pearl River basin in South China

Jun Niu, Ji Chen*

Department of Civil Engineering, The University of Hong Kong, Pokfulam, Hong Kong, China

Received 13 April 2009; revised 22 April 2010; accepted 30 April 2010

numerical modeling

Journal of Hydrology 420–421 (2012) 319–328

Contents lists available at SciVerse ScienceDirect

Journal of Hydrology

journal homepage: www.elsevier.com/locate/jhydrol

Advancing representation of hydrologic processes in the Soil and Water Assessment Tool (SWAT) through integration of the TOPographic MODEL (TOPMODEL) features

Ji Chen [a,*], Yiping Wu [a,b]

[a] *Department of Civil Engineering, The University of Hong Kong, Pokfulam, Hong Kong, China*

[b] *ASRC Research and Technology Solutions, U.S. Geological Survey (USGS) Earth Resources Observation and Science (EROS) Center, Sioux Falls, SD 57198, USA*

Available online at www.sciencedirect.com
ScienceDirect
Journal of Hydro-environment Research 4 (2010) 279–288
Journal of Hydro-environment Research
www.elsevier.com/locate/jher
Research paper

Terrestrial hydrological features of the Pearl River basin in South China

Jun Niu, Ji Chen*
Department of Civil Engineering, The University of Hong Kong, Pokfulam, Hong Kong, China

Received 13 April 2009; revised 22 April 2010; accepted 30 April 2010

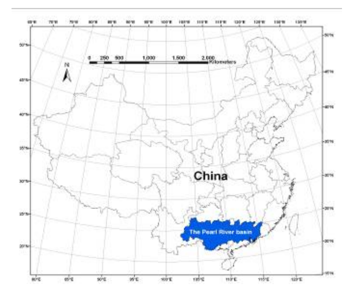

The Pearl River basin

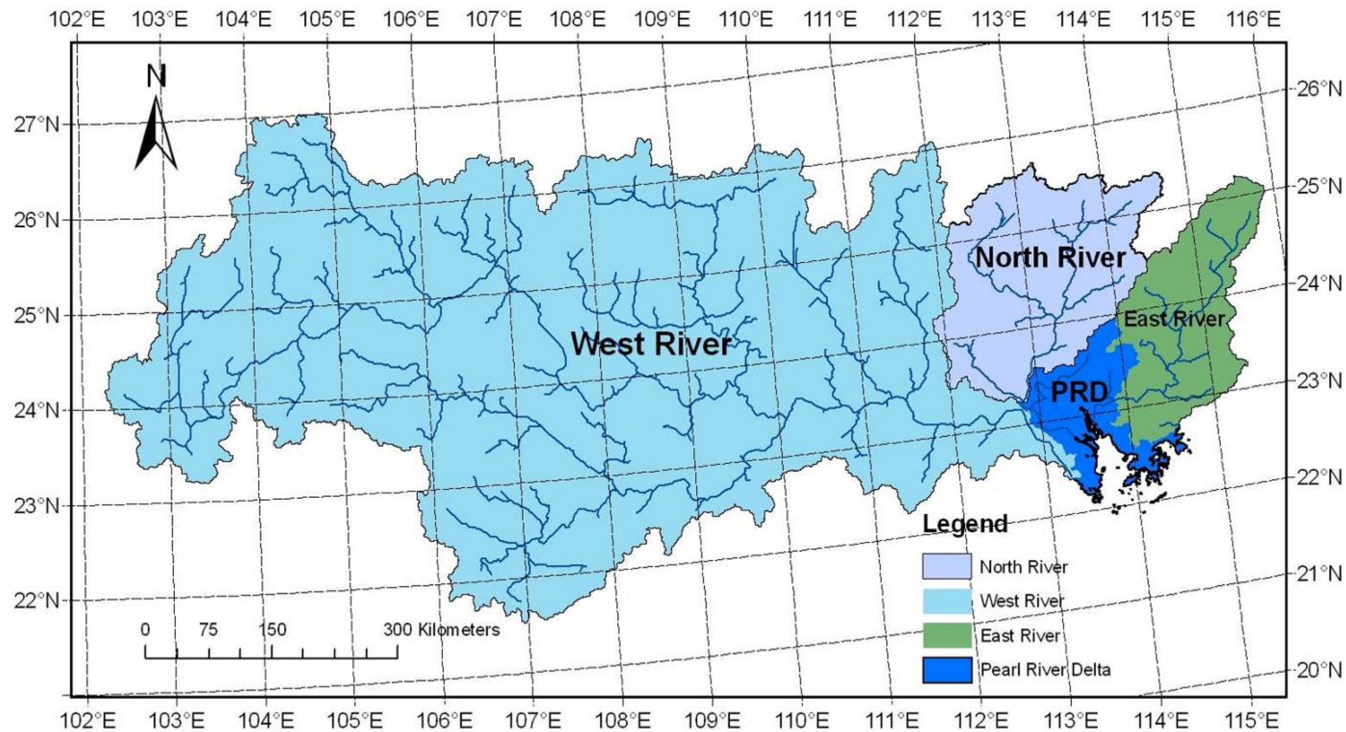

- Total basin area 453,690 km^2
- Average Annual precipitation 1477mm/yr
- Four river systems: West River, North River, East River, Pearl River Delta

Variable Infiltration Capacity (VIC) Macroscale Hydrological Model

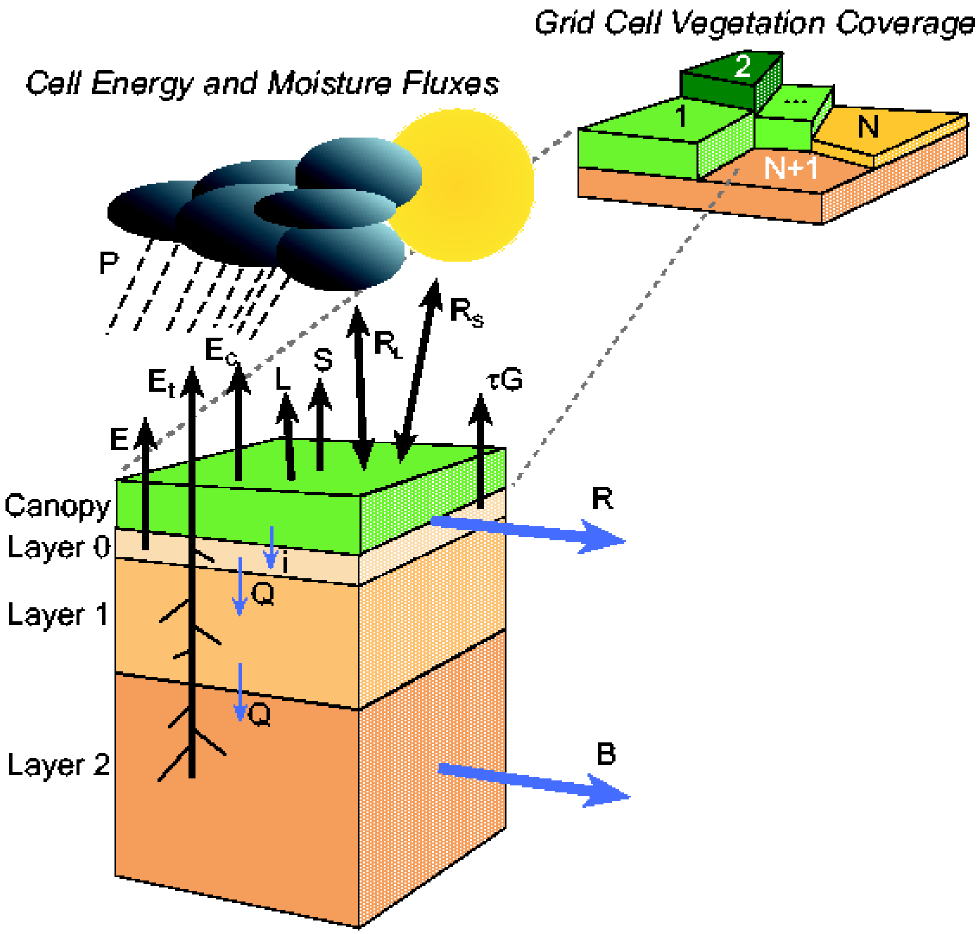

From: http://www.hydro.washington.edu/Lettenmaier/Models/VIC

- The VIC-NL model represents surface and subsurface hydrologic processes on a spatially distributed (grid cell) basis.
- Energy and water balance terms are computed independently for each coverage class (vegetation and bare soil) present in the model.
- Processes governing the flux and storage of water and heat in each cell-sized system of vegetation and soil structure include

evaporation from the soil layers (E)
evapotranspiration (E_t)
canopy interception evaporation (E_c)
latent heat flux (L)
sensible heat flux (S)
longwave radiation (R_L)
shortwave radiation (R_S)
ground heat flux (G)
infiltration (i) **percolation (Q)**
runoff (R) **baseflow (B)**

Run the VIC model over Pearl River basin

- Define area of interest

DEM: GIS with HYDRO 1K data Grid resolution: $1^\circ \times 1^\circ$

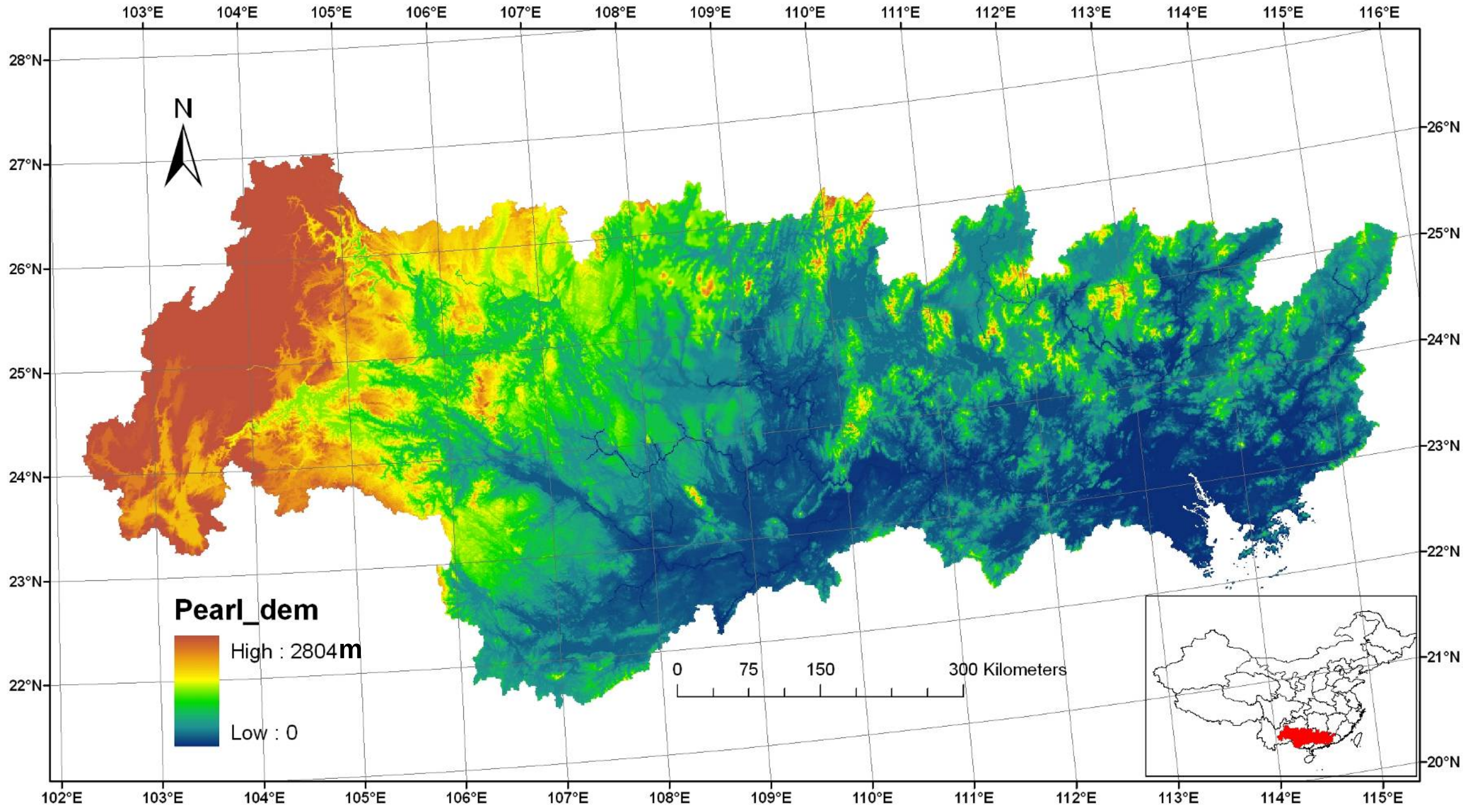

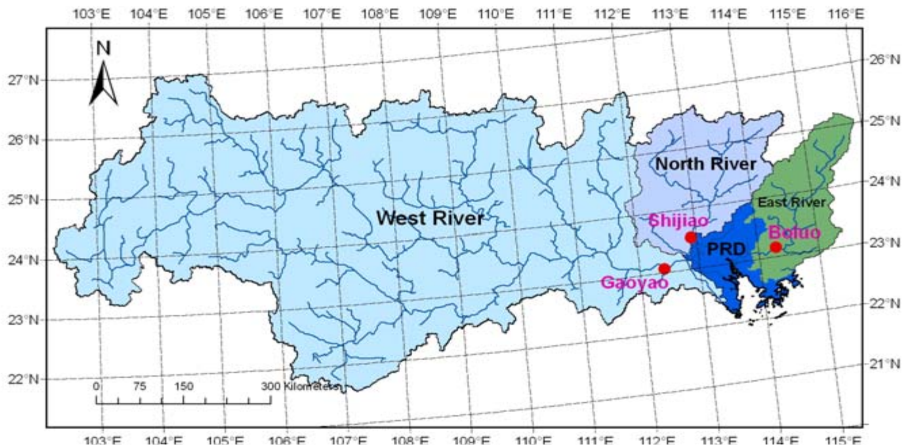

Comparison of Simulations and Observations at Gaoyao Station of the West River

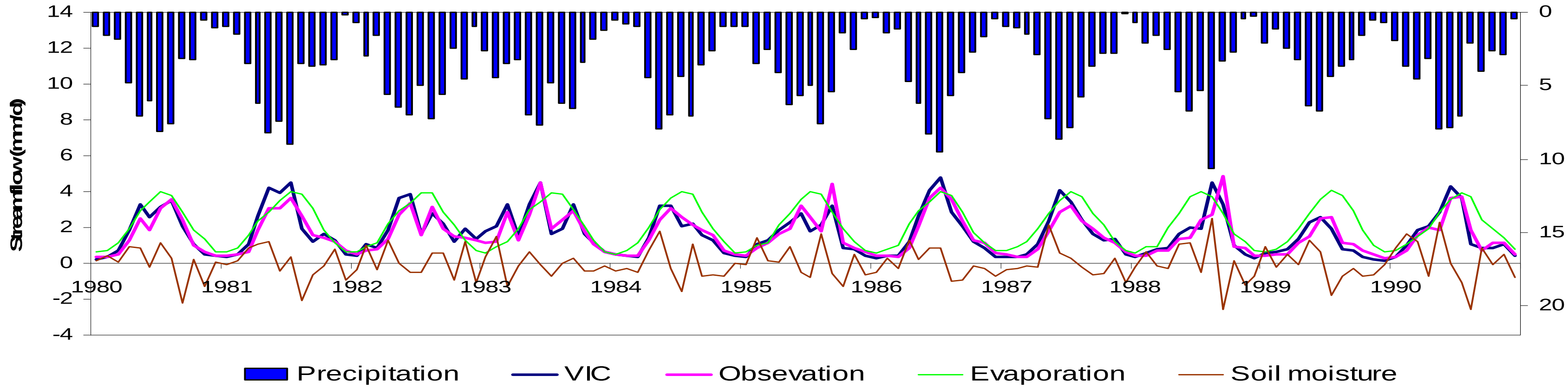

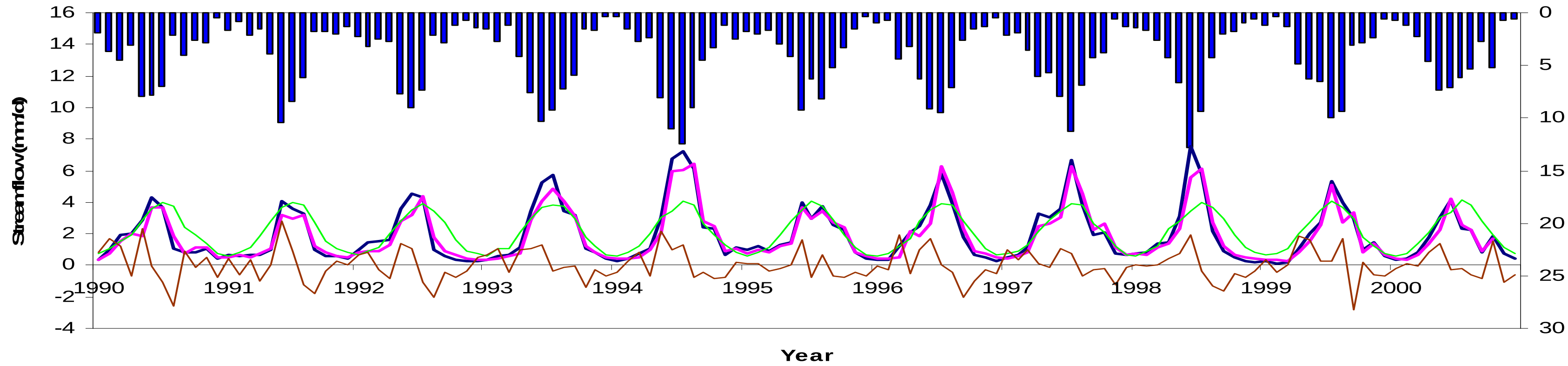

Relative Bias=0.05

R^2=0.908

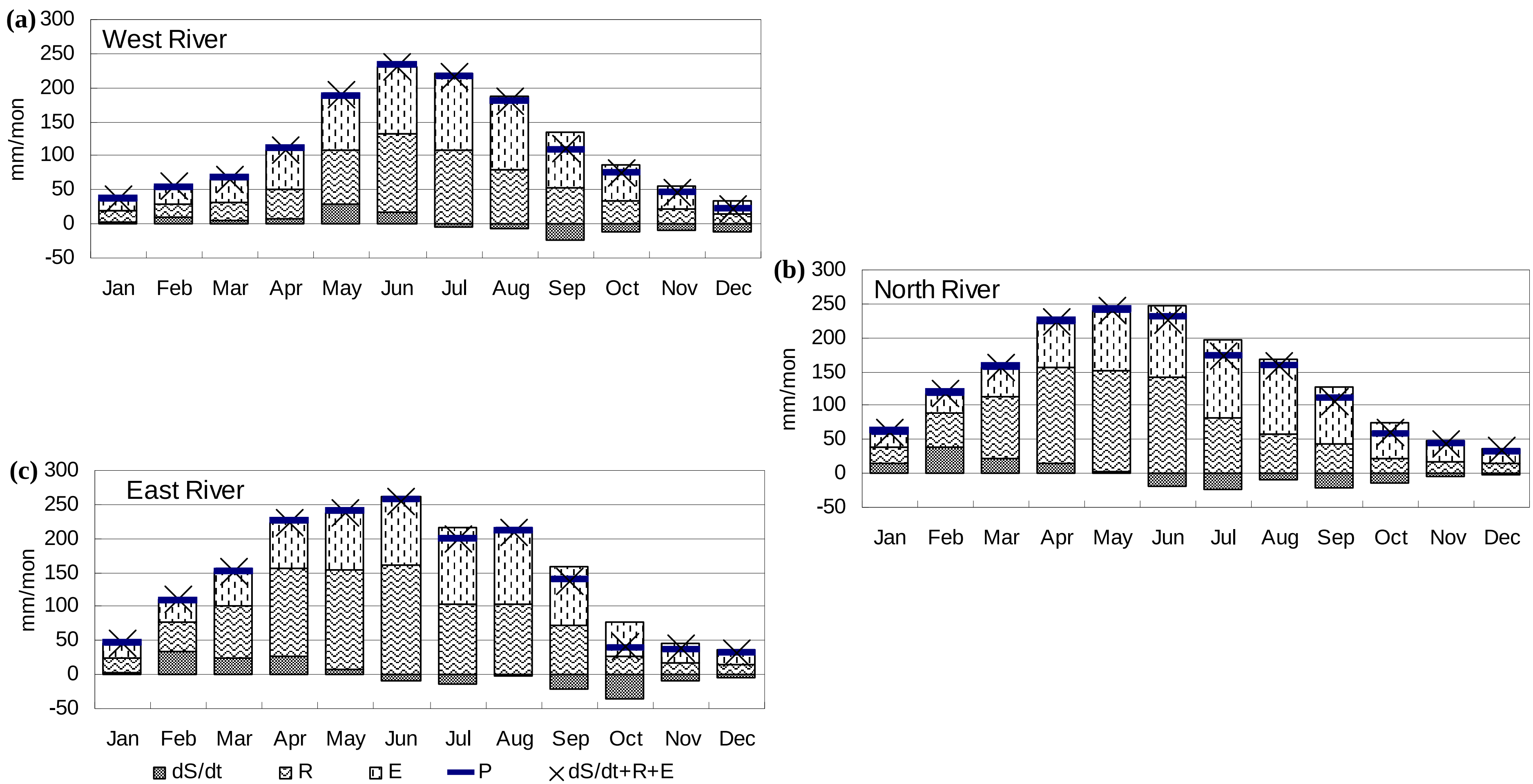

Monthly observed precipitation (noted as *P*) and hydrological components from the VIC simulation for three tributaries of the Pearl River over the period 1980 to 2000. The notation *dS/dt* represents the monthly change of soil water storage. *R* and *E* represent the monthly average of model simulated runoff and evapotranspiration, respectively. The cross mark refers to the sum of *dS/dt*, *R* and *E*.

Journal of Hydrology 420–421 (2012) 319–328

Contents lists available at SciVerse ScienceDirect

Journal of Hydrology

journal homepage: www.elsevier.com/locate/jhydrol

Advancing representation of hydrologic processes in the Soil and Water Assessment Tool (SWAT) through integration of the TOPographic MODEL (TOPMODEL) features

Ji Chen[a,*], Yiping Wu[a,b]

[a] Department of Civil Engineering, The University of Hong Kong, Pokfulam, Hong Kong, China
[b] ASRC Research and Technology Solutions, U.S. Geological Survey (USGS) Earth Resources Observation and Science (EROS) Center, Sioux Falls, SD 57198, USA

Hydrologic cycle in SWAT (Soil and Water Assessment Tool)

$$SW_t = SW_o + \sum_{i=1}^{t} (R_{day,i} - Q_{surf,i} - E_{act,i} - W_{seep,i} - Q_{lat,i}) \quad \text{(mm/d)}$$

(Neitsch *et al.* 2005)

Soil profile

Groundwater

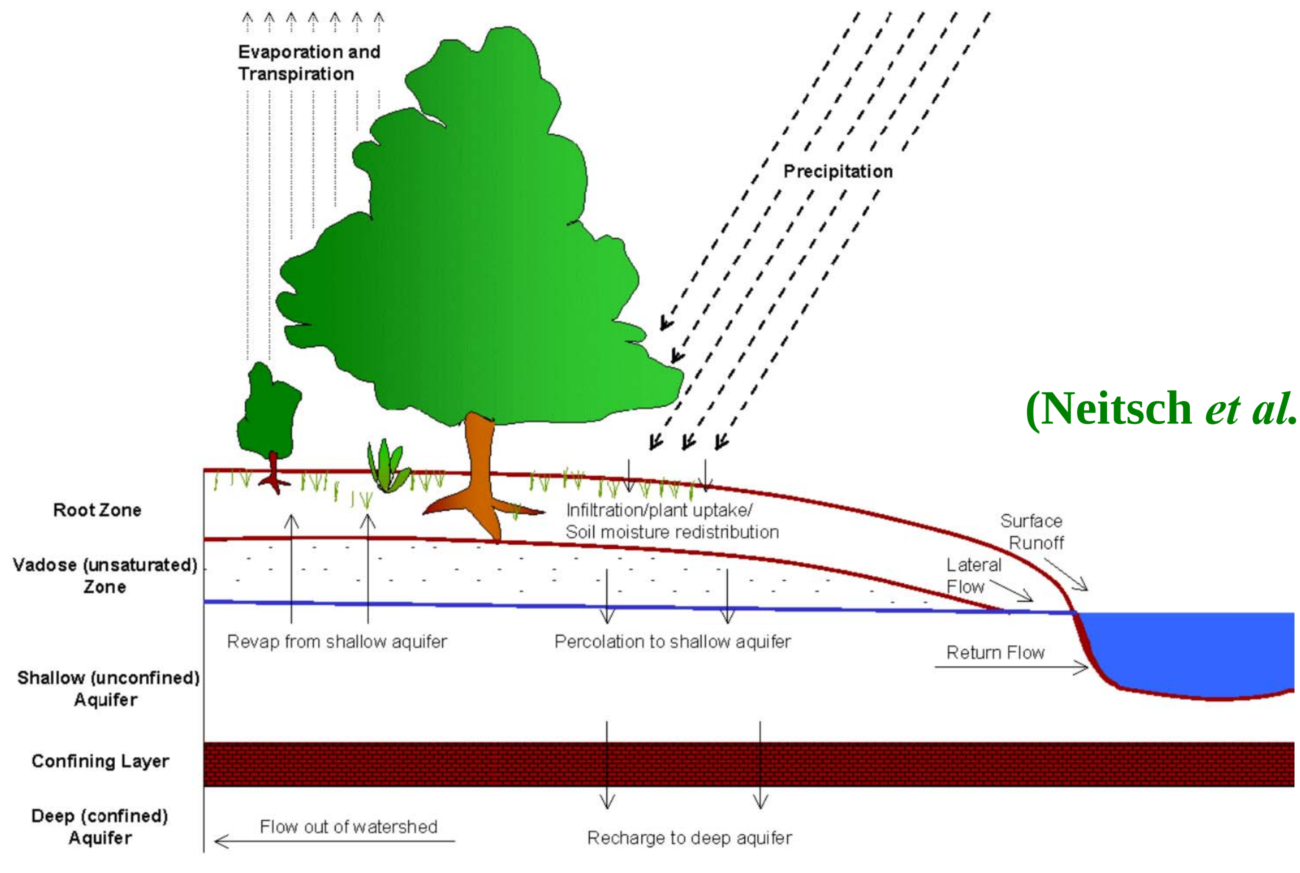

Four hydrological processes in SWAT

Hydrological Processes	Calculation and Parameters involved		Limitations
Overland flow	$Q_{surf} = \frac{\left(R_{day} - I_a\right)^2}{\left(R_{day} - I_a + S_a\right)}$	S_a	without considering direct overland flow from saturated area
Revap	$W_{revap,mx} = \beta_{revap} \cdot E_0$	β_{revap}	to be calibrated time invariant spatially unchanged
Baseflow	$Q_{b,i} = Q_{b,i-1} \cdot e^{-\alpha_{gw} \cdot \Delta t} + W_r \cdot (1 - e^{-\alpha_{gw} \cdot \Delta t})$	α_{gw}	to be calibrated $f\ (W_r)$
Percolation to deep aquifer	$w_{deep,mx} = \beta_{deep} w_{rchrg}$	β_{deep}	to be calibrated this amount of water is returned to hydrologic cycle only by pumping

Relationship Between the Saturated Area and Water Table Depth

- **Map of saturated areas showing expansion during a single rainstorm.** **(Dunne and Leopold, 1978)**

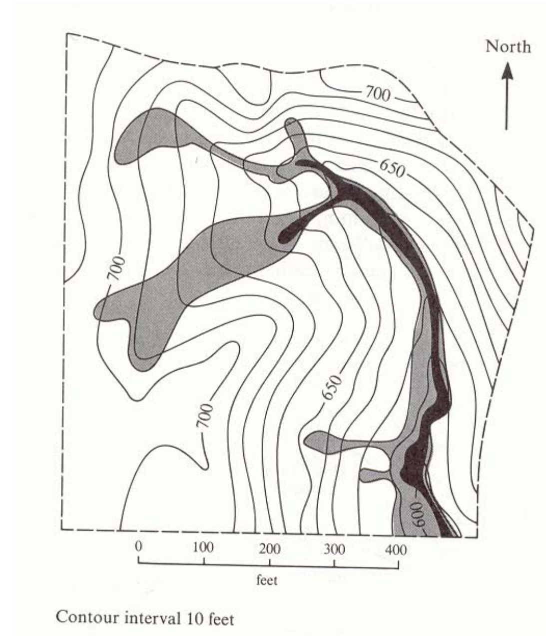

- **Saturated fraction** $fr_{sat} = \dfrac{A_c}{A} = f(\lambda, \bar{z}, \xi)$

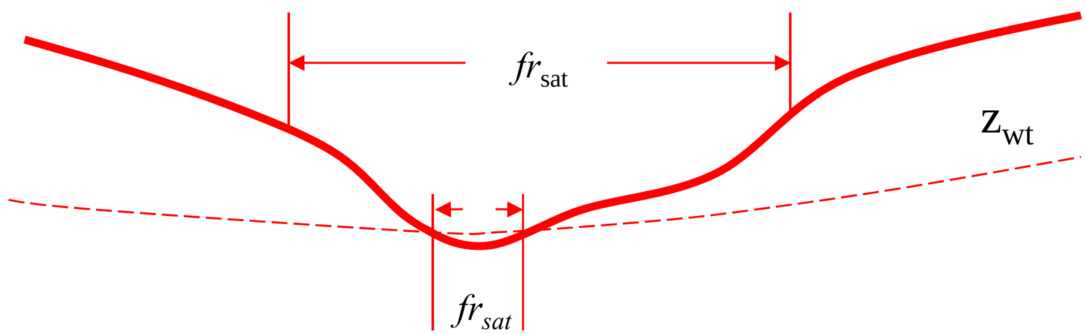

- **Topographic Index** $= \ln \dfrac{a}{\tan \beta}$

a is the upstream contributing area

$\tan\beta$ is the local slope

(Beven and Kirkby 1979)

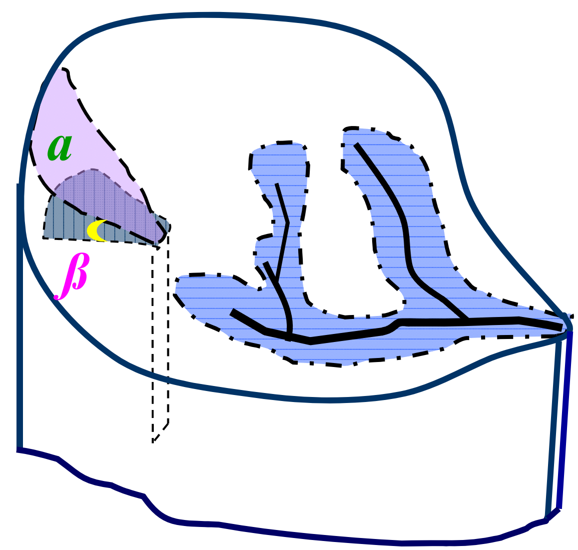

Comparison of revap

Scenario	Model	Revap	Comparison period
I	SWAT	*f* (PET)	Jan and Mar Mid Sep
II	SWAT-TOPMODEL	*f* (PET, fr_{sat})	

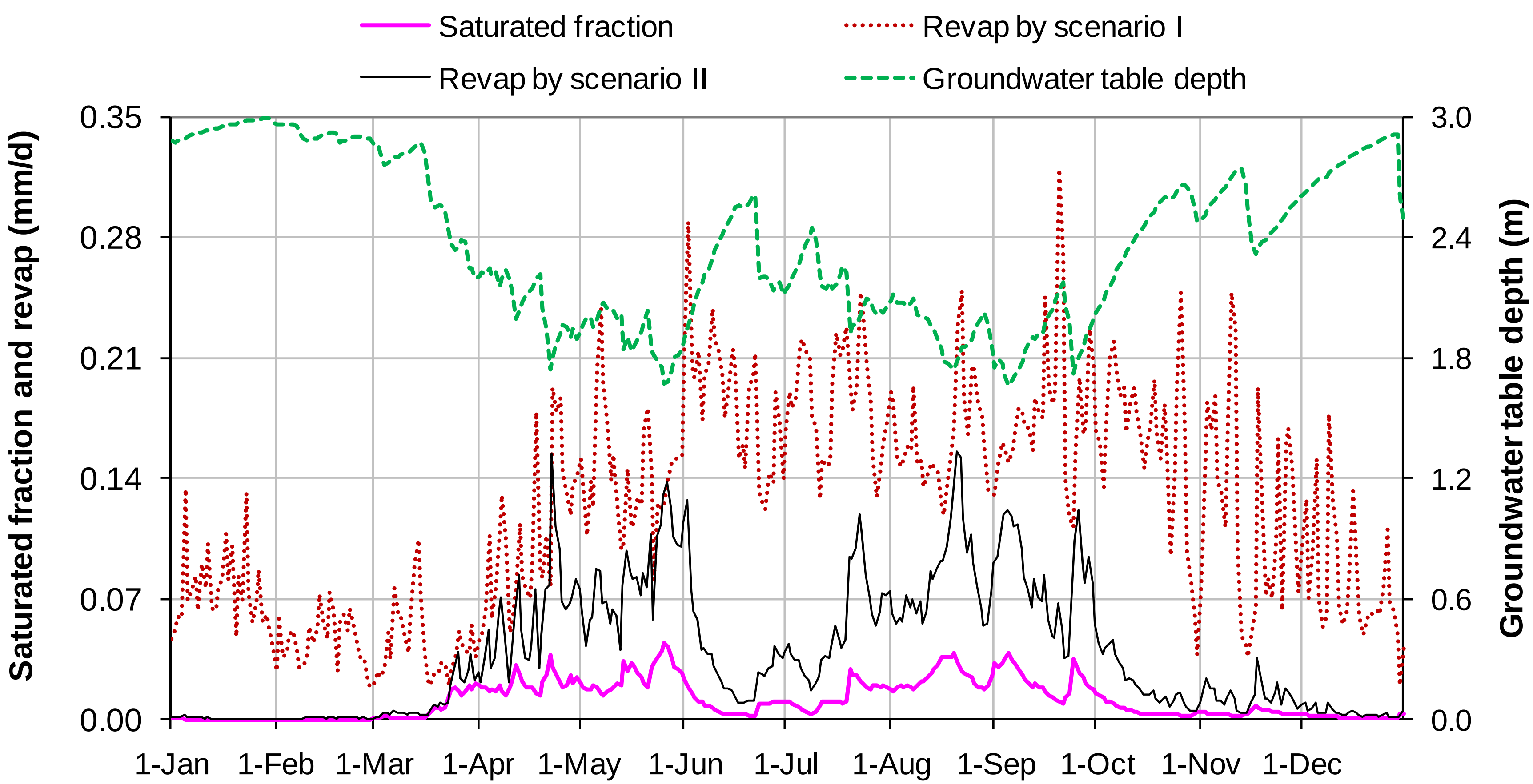

Computers & Geosciences 36 (2010) 1427–1435

Contents lists available at ScienceDirect

Computers & Geosciences

journal homepage: www.elsevier.com/locate/cageo

A modified binary tree codification of drainage networks to support complex hydrological models

Tiejian Li [a,b], Guangqian Wang [a], Ji Chen [b,*]

[a] State Key Laboratory of Hydroscience and Engineering, Tsinghua University, Beijing 100084, China
[b] Department of Civil Engineering, The University of Hong Kong, Hong Kong, China

computational technology

Environmental Modelling & Software 26 (2011) 1736–1746

Contents lists available at ScienceDirect

Environmental Modelling & Software

journal homepage: www.elsevier.com/locate/envsoft

Dynamic parallelization of hydrological model simulations

Tiejian Li [a,b], Guangqian Wang [a], Ji Chen [b,*], Hao Wang [a,1]

[a] State Key Laboratory of Hydroscience and Engineering, Tsinghua University, Beijing, 100084, China
[b] Department of Civil Engineering, The University of Hong Kong, Pokfulam, Hong Kong, China

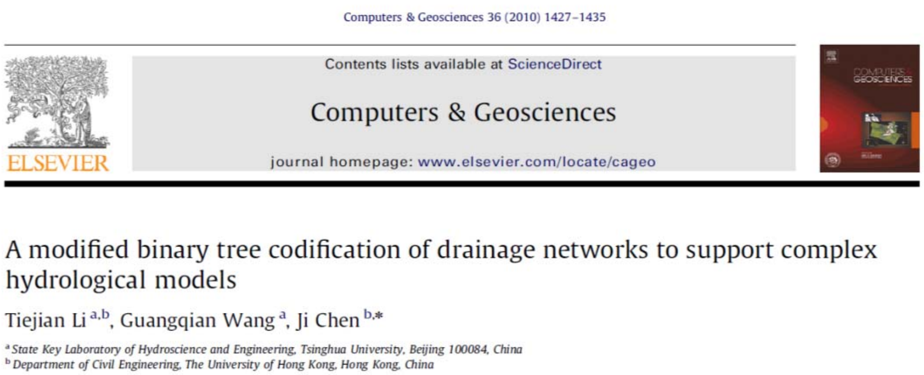

Computers & Geosciences 36 (2010) 1427–1435

Contents lists available at ScienceDirect

Computers & Geosciences

journal homepage: www.elsevier.com/locate/cageo

A modified binary tree codification of drainage networks to support complex hydrological models

Tiejian Li [a,b], Guangqian Wang [a], Ji Chen [b,*]

[a] State Key Laboratory of Hydroscience and Engineering, Tsinghua University, Beijing 100084, China

[b] Department of Civil Engineering, The University of Hong Kong, Hong Kong, China

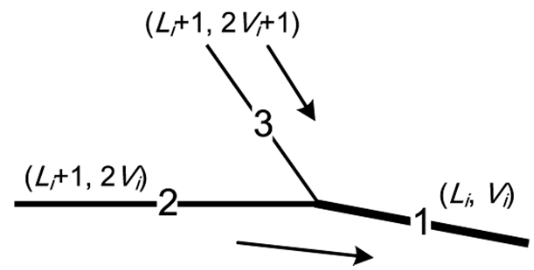

A typical section of a drainage network

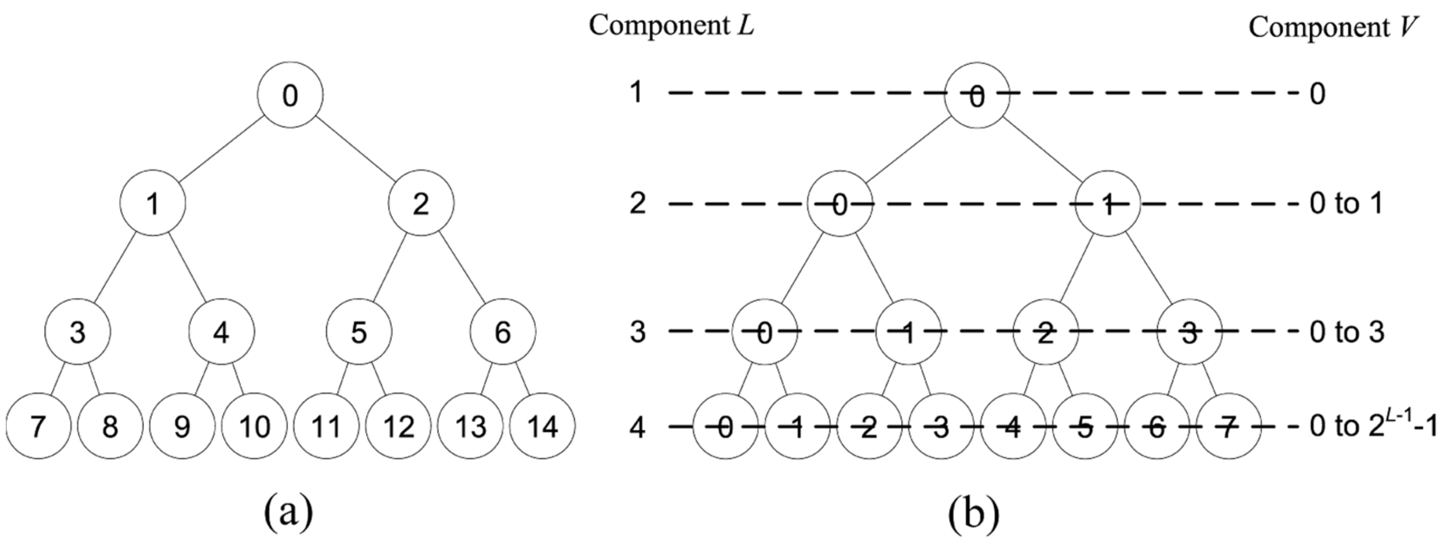

(a) Array-based binary tree. Connected nodes can be directly located by sequential indices. (b) Two-component code for a binary tree. Component *L* indicates level of a node in tree, and component *V* (in circles denoting nodes) indicates index of a node in its level *L* and grows from left to right from 0 to 2^{L-1}-1.

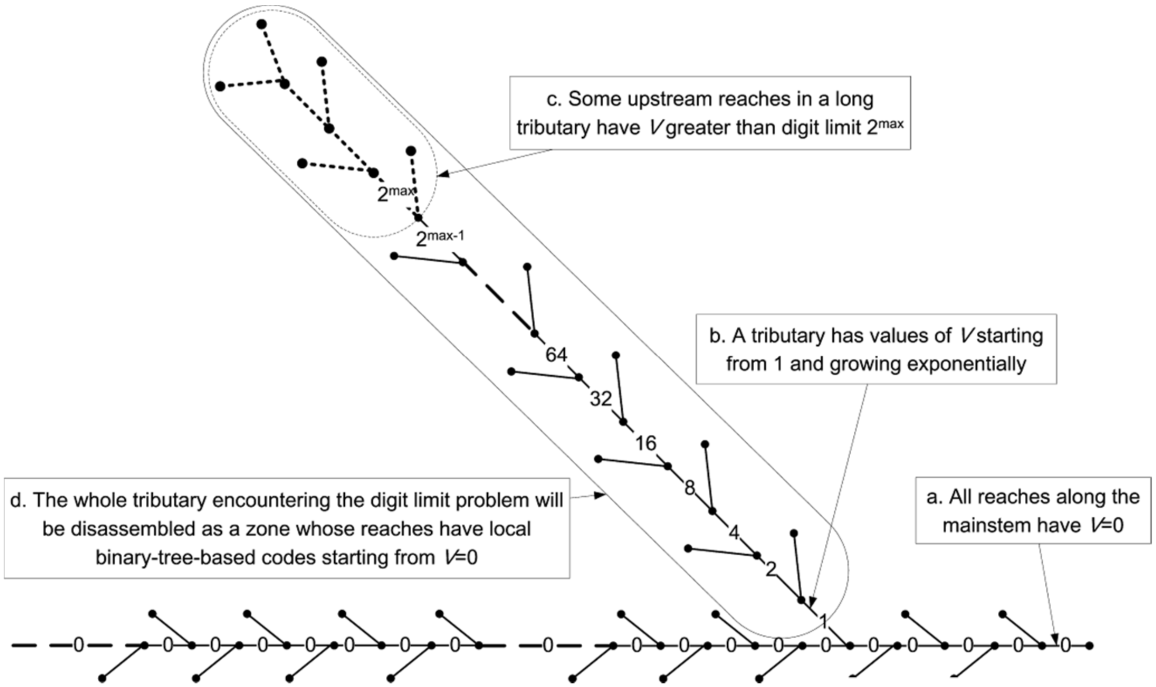

Digit overflow problem of binary-tree-based codification. Values of component *V* grow exponentially in a tributary; if a tributary is sufficiently long, component *V* will exceed a digit limit 2^{max}, which is defined by the computer system or programming language. Therefore, a long tributary is disassembled as a zone with own binary-tree-based codes to avoid digit overflow.

Hierarchically coded zones in a drainage network. Each zone has its order and sequence, which are recomposed to a unitary zone index. Reaches via which higher order zones converge to a lower order one are recorded in (*Z*, *L*, *V*) (e.g., (0, 15, 1)) to make river reaches in drainage network connect as a whole.

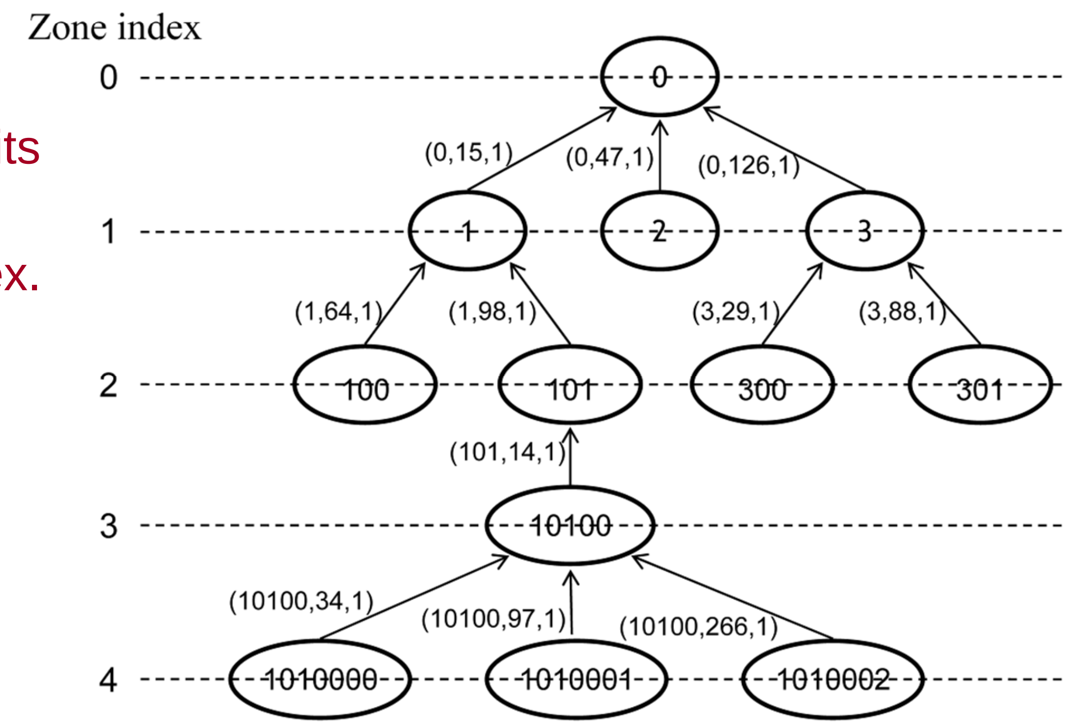

Hierarchical structure of the Yellow River basin. (a) Shaded region shows extent of coarse sediment source area in the Middle Yellow River basin. (b) Main tributaries covering coarse sediment source area are shown with zone indices, and the Chabagou River basin locates near doted region. (c) Drainage network of Chabagou River basin is shown. (d) A part of Chabagou drainage network is displayed to show connection between map and data records.

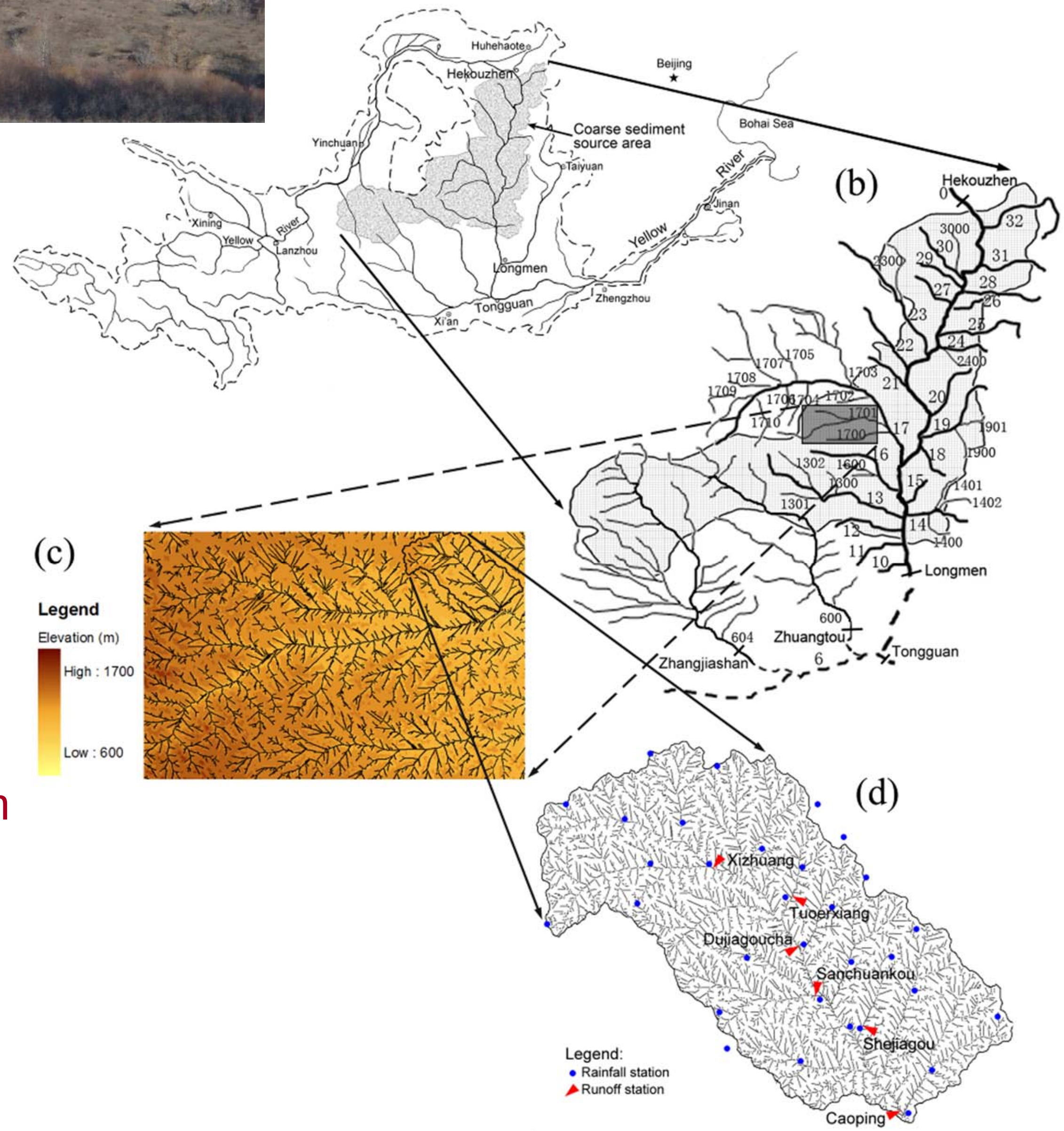

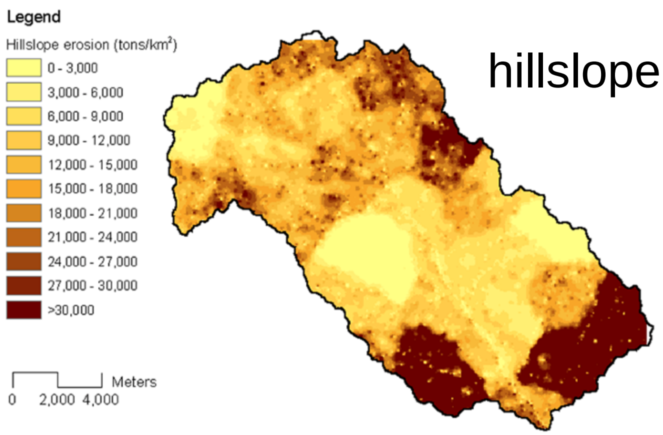

hillslope erosion

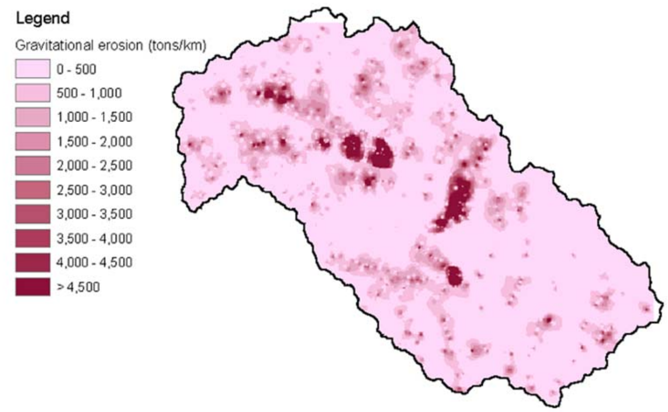

gravitational (i.e. gully) erosion

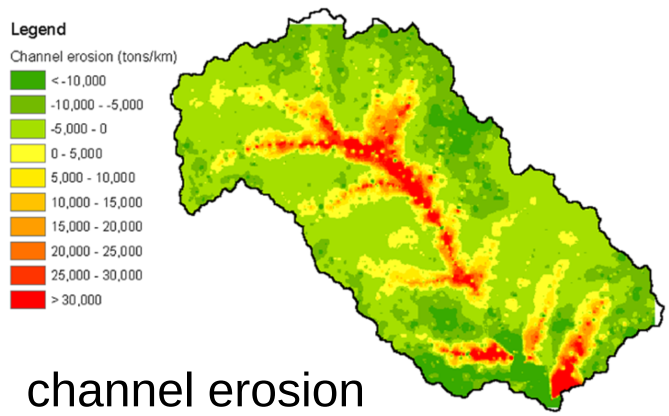

channel erosion

Simulated distributions of soil erosion from different sources

Environmental Modelling & Software 26 (2011) 1736–1746

Contents lists available at ScienceDirect

Environmental Modelling & Software

journal homepage: www.elsevier.com/locate/envsoft

Dynamic parallelization of hydrological model simulations

Tiejian Li[a,b], Guangqian Wang[a], Ji Chen[b,*], Hao Wang[a,1]

[a] State Key Laboratory of Hydroscience and Engineering, Tsinghua University, Beijing, 100084, China
[b] Department of Civil Engineering, The University of Hong Kong, Pokfulam, Hong Kong, China

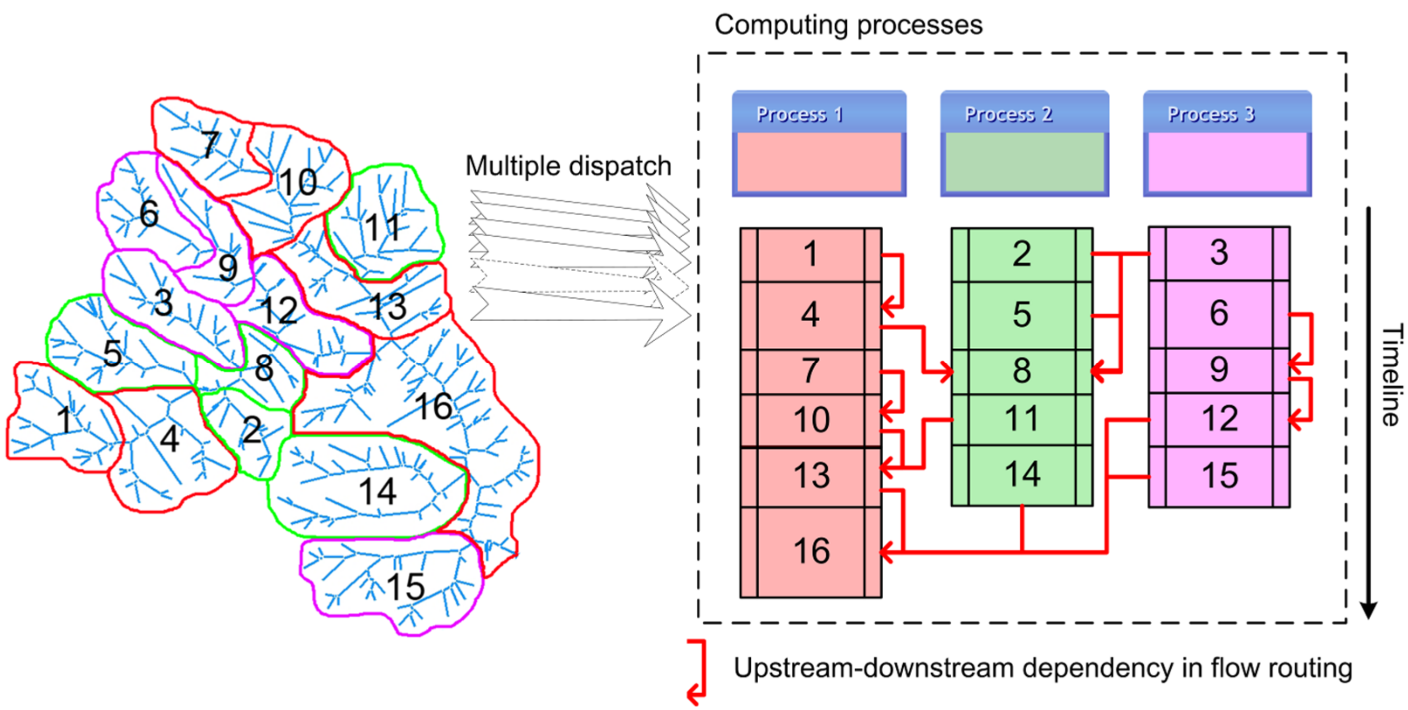

The diagram of dynamic decomposition of a drainage network, and the subbasins with the boundary line colors of brown, green and pink are dispatched to the computing processes 1, 2 and 3, respectively

The flowchart for dynamic decomposition of a basin.

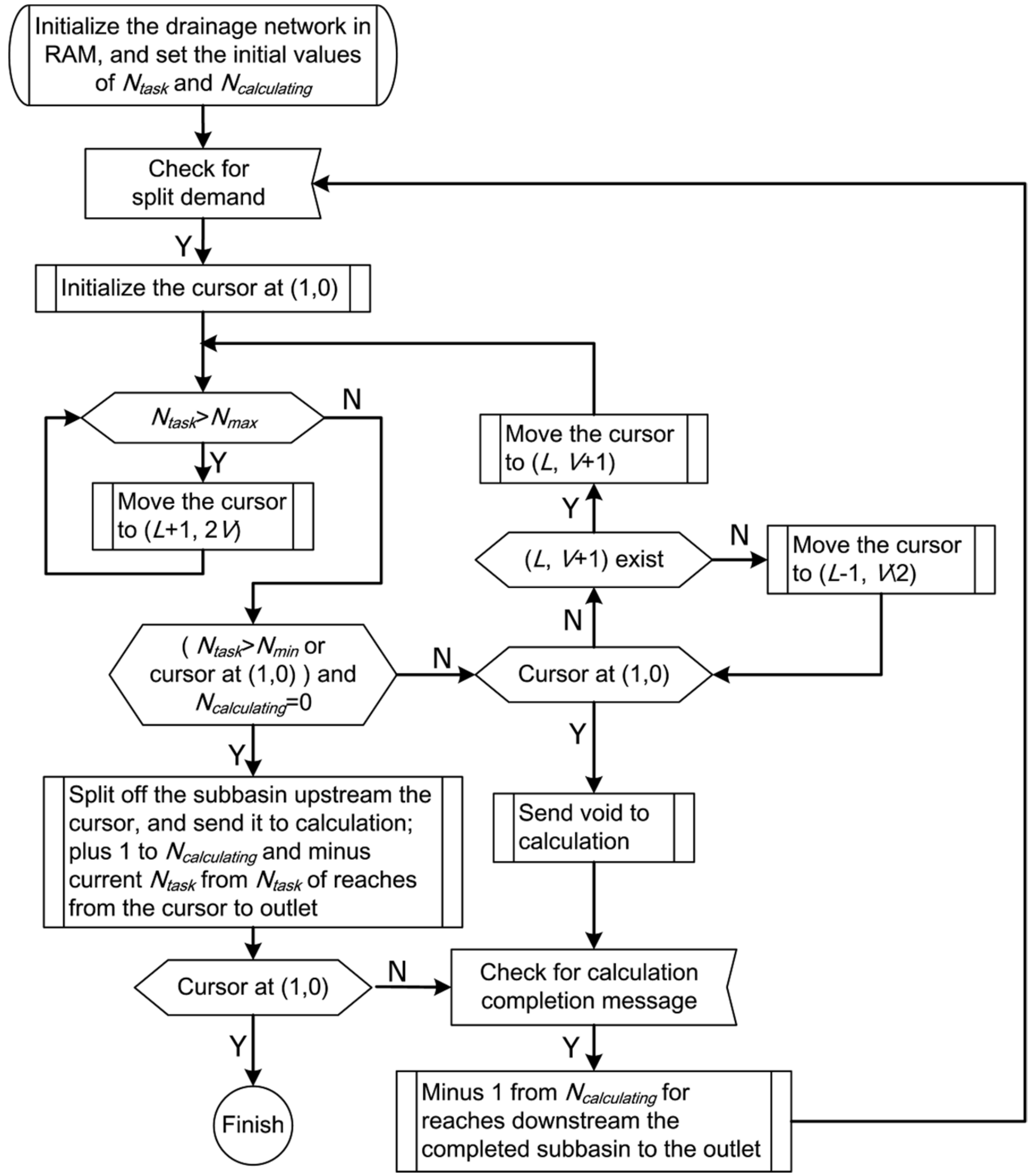

Flowchart of the execution of master, slave and data transfer processes, in which the bold arrow lines denote the transfer of message and/or data.

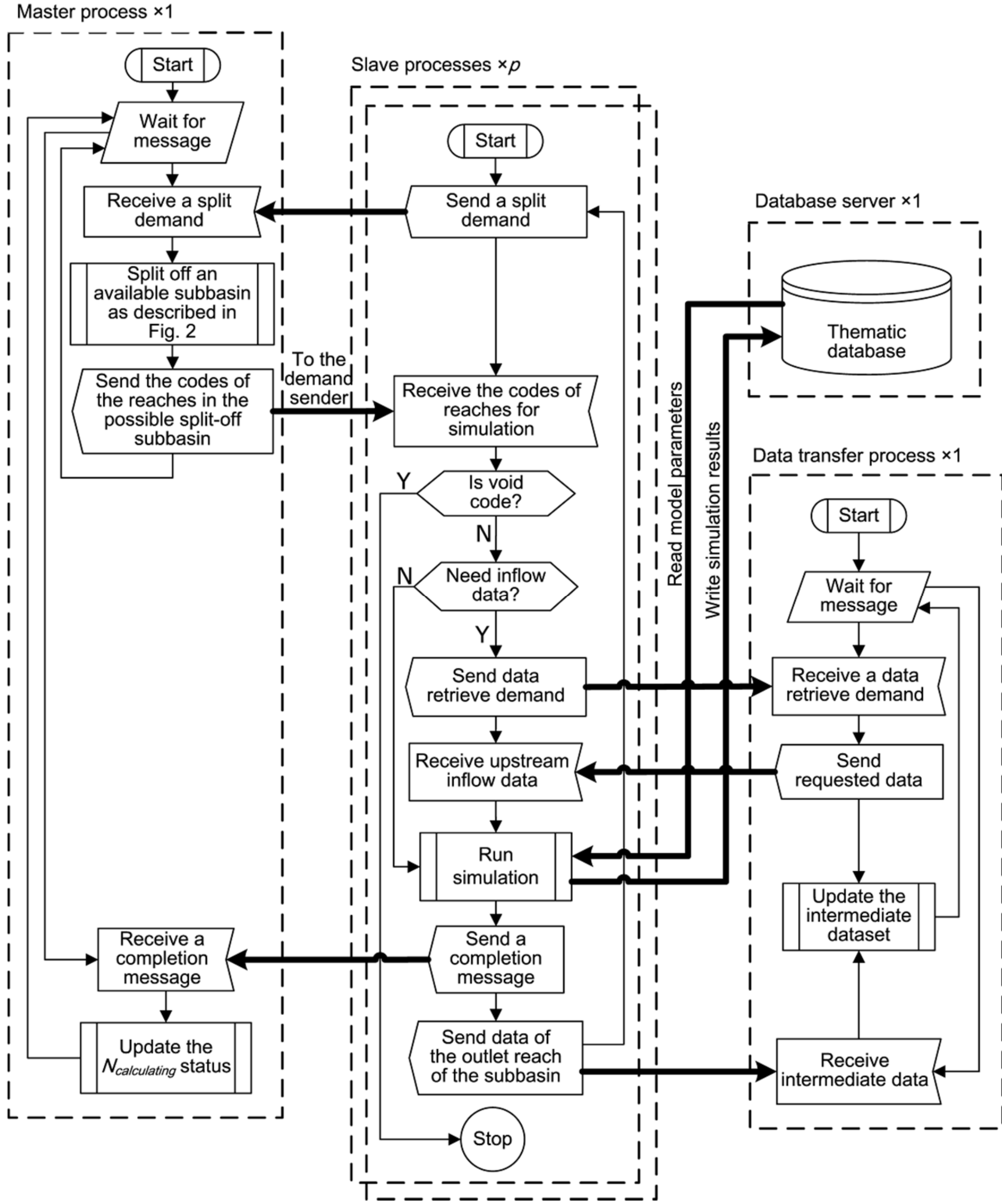

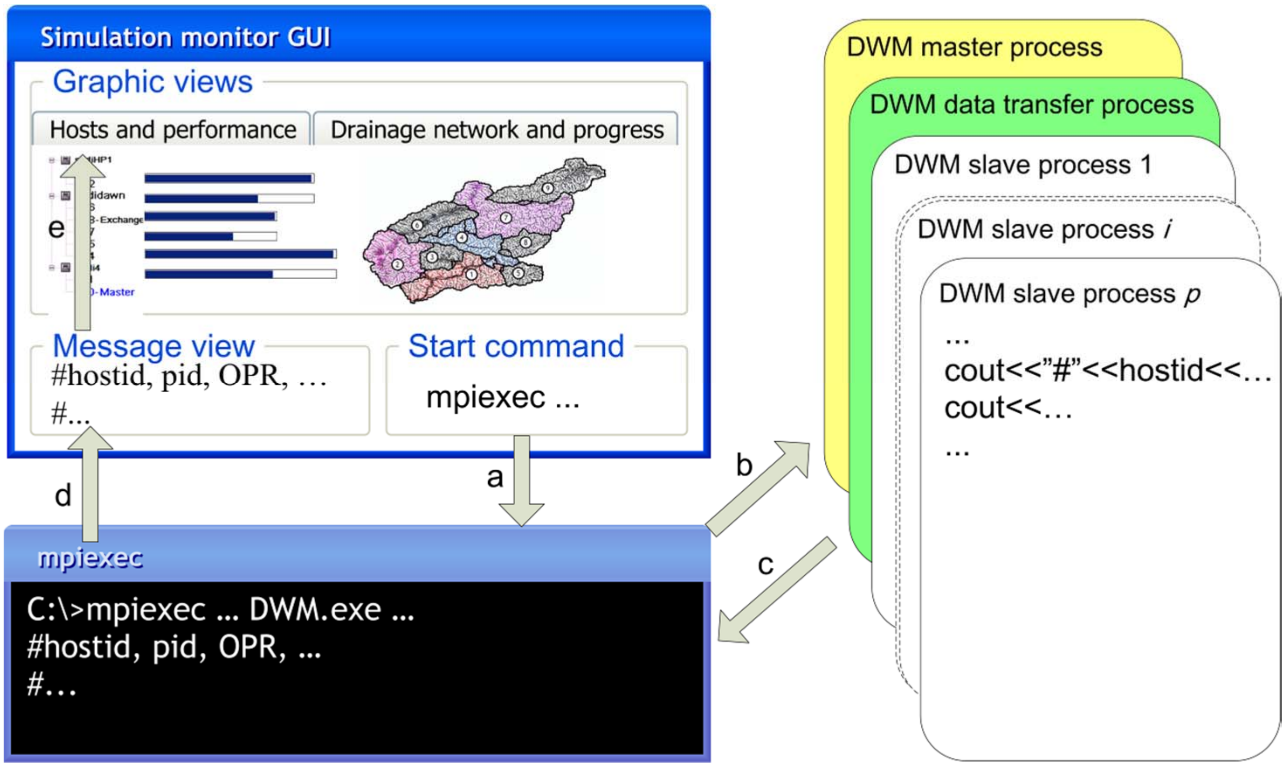

Schematic of the realization of the simulation monitor with graphical user interface (GUI), MPI control. The passes of commands and messages are: a) the GUI sends a mpiexec command to start the MPI running environment, b) the mpiexec command starts the DWM.main program in multiple processes, c) messages from DWM.main processes are gathered by mpiexec and written in the Windows command console, d) messages in the command console are passed to the GUI via anonymous pipe, and e) Messages are interpreted so as to draw the chart and map to show the performance and progress of simulation.

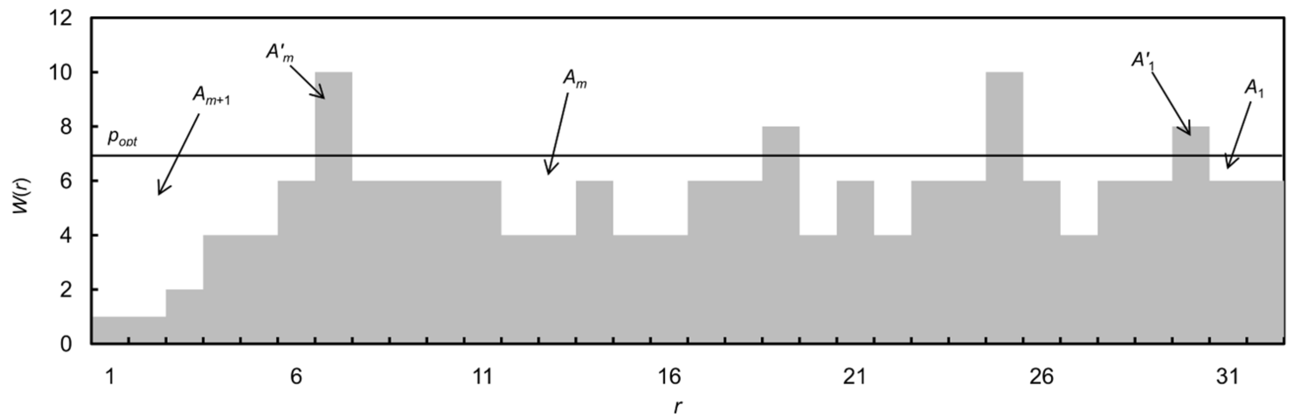

The topological width function, which is derived from a corresponding coarse resolution drainage network and is used to reflect the inter connection of subbasins. The straight line reflecting the number of *p* slave processes.

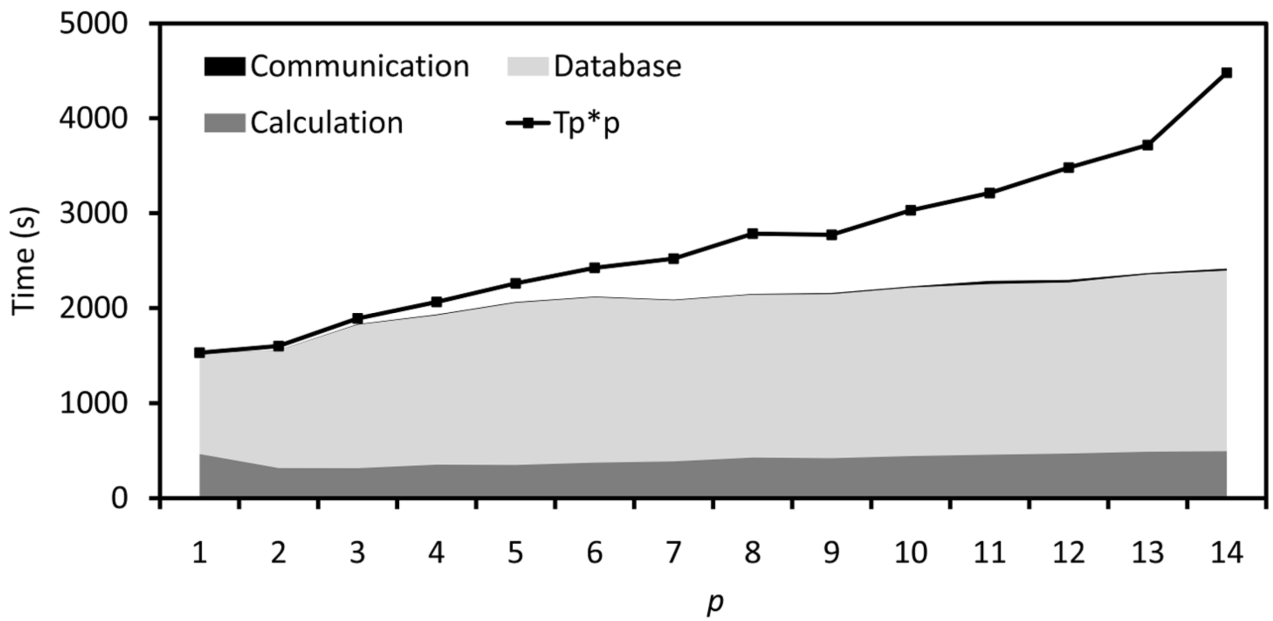

Different portions of computer time and the value of the total computation capacity (i.e. *Tp**p*) for the different number of slave computing processes.

Thank you !